A 42

AFML-TR-75-178

DEVELOPMENT OF HIGHLY ORIENTED POLYMERS WITH IMPROVED MECHANICAL PROPERTIES

INSTITUTE OF POLYMER SCIENCE
THE UNIVERSITY OF AKRON
AKRON, OHIO 44325

DECEMBER, 1975

TECHNICAL REPORT AFML-TR-75-178
FINAL REPORT FOR PERIOD JUNE 1973 – JUNE 1975

AIR FORCE MATERIALS LABORATORY
AIR FORCE WRIGHT AERONAUTICAL LABORATORIES
Air Force Systems Command
Wright-Patterson Air Force Base, Ohio 45433

11

NOTICE

When Government drawings, specifications, or other data are used for any purpose other than in connection with a definitely related Government procurement operation, the United States Government thereby incurs no responsibility nor any obligation whatsoever; and the fact that the government may have formulated, furnished, or in any way supplied the said drawings, specifications or other data, is not to be regarded by implication or otherwise as in any manner licensing the holder or any other person or corporation, or conveying any rights or permission to manufacture, use, or sell any patented invention that may in any way be related thereto.

This report has been reviewed by the Information Office (OI) and is releasable to the National Technical Information Service (NTIS). At NTIS, it will be available to the general public, including foreign nations.

R. L. Van Deusen
Chief, Polymer Branch
Nonmetallic Materials Division
Air Force Materials Laboratory

Anthony Wereta, Jr., Capt, USAF
Project Scientist
Nonmetallic Materials Division
Air Force Materials Laboratory

Copies of this report should not be returned unless return is required by security considerations, contractual obligations, or notice on a specific document.

AIR FORCE - 10 MAY 76 - 100

UNCLASSIFIED

SECURITY CLASSIFICATION OF THIS PAGE *(When Data Entered)*

REPORT DOCUMENTATION PAGE		READ INSTRUCTIONS BEFORE COMPLETING FORM
1. REPORT NUMBER AFML-TR-75-178	2. GOVT ACCESSION NO.	3. RECIPIENT'S CATALOG NUMBER
4. TITLE *(and Subtitle)* "DEVELOPMENT OF HIGHLY ORIENTED POLYMERS WITH IMPROVED MECHANICAL PROPERTIES"		5. TYPE OF REPORT & PERIOD COVERED 6. PERFORMING ORG. REPORT NUMBER
7. AUTHOR(s) Meinecke, Eberhard A. McIntyre, Donald		8. CONTRACT OR GRANT NUMBER(s) F33615-73-C-5113
9. PERFORMING ORGANIZATION NAME AND ADDRESS Air Force Materials Laboratory Air Force Systems Command Wright Patterson AFB, Ohio 45433		10. PROGRAM ELEMENT, PROJECT, TASK AREA & WORK UNIT NUMBERS
11. CONTROLLING OFFICE NAME AND ADDRESS Air Force Materials Laboratory Wright-Patterson AFB, Ohio 45433		12. REPORT DATE December 1975 13. NUMBER OF PAGES
14. MONITORING AGENCY NAME & ADDRESS*(if different from Controlling Office)*		15. SECURITY CLASS. *(of this report)* Unclassified 15a. DECLASSIFICATION/DOWNGRADING SCHEDULE

16. DISTRIBUTION STATEMENT *(of this Report)*

Approved for Public Release; Distribution Unlimited.

17. DISTRIBUTION STATEMENT *(of the abstract entered in Block 20, if different from Report)*

18. SUPPLEMENTARY NOTES

19. KEY WORDS *(Continue on reverse side if necessary and identify by block number)*

20. ABSTRACT *(Continue on reverse side if necessary and identify by block number)*

Highly oriented crystalline polymer films are prepared in several different ways. In many cases the mechanical properties of the film are examined experimentally and related to the theoretical expectations of strengths and moduli.

The first general method adopted in this study to produce oriented polymer films involves the crystallization of polyethylenes in dulute solutions under shear. The data indicate a trend towards

DD FORM 1 JAN 73 1473 EDITION OF 1 NOV 65 IS OBSOLETE

UNCLASSIFIED

SECURITY CLASSIFICATION OF THIS PAGE *(When Data Entered)*

greater orientation with increased shear rate; however, the films lack good physical integrity. Consequently the mechanical properties are low compared to theoretical expectations.

The second general method adopted involves the simultaneous application of a shear field and high pressure on dilute solutions of polyethylene in a top-stirred high pressure reactor kept at constant stirring rates. The pressures varied from atmospheric to 400C psi, and the stirring rate ranged from 110 to 380 rpm. The films had greater physical integrity in this experiment than in the first method, but the dependence of the mechanical properties on the pressure and stirring rate is not clear. Although better orientation can on occasion be obtained, further work is necessary to clarify the functional dependence of mechanical properties, reactor conditions, and crystal orientation.

A third general method of obtaining highly oriented polymer film uses a very rigid polymer backbone structure. Semi-rigid cellulosic polymers and very stiff poly-(n-alkyl isocyanate) and poly-(-benzyl L-glutanate) films are described. The films are prepared using both ultra-thin film casting and melt extrusion. The orientation of these very stiff chains, particularly poly-(n-hexyl) isocyanate, is found to be extremely high. Only small amounts of these polymers are available. However, the high crystallite orientation of these polymers suggests that they are more likely to produce desirable mechanical properties. Further work with these polymers is recommended.

TABLE OF CONTENTS

TABLE OF CONTENTS (Concluded)

LIST OF ILLUSTRATIONS

LIST OF ILLUSTRATIONS (cont'd)

LIST OF ILLUSTRATIONS (Concluded)

LIST OF TABLES

1. PREPARATION OF HIGHLY ORIENTED POLYMERIC MATERIALS

1.1 Introduction

The mechanical properties of crystalline polymers are related to the chain conformation and crystal orientation. Crystallization of a polymer with a random chain conformation yields a material with random crystal orientations and isotropic behavior. Application of a tensile load causes conformational changes, high elongation, and the load will be supported by only a fraction of the primary bonds. (See Fig. 1.)

If the chains are fully extended so that their deformation is no longer governed by conformational changes due to bond rotation, then the application of a tensile load to the fully extended chains would be supported by the primary bonds and the elongation will be very small since it will result only from the bending of these (normally 109^0) bonds, as for example in the case of polyethylene. If the crystal structures resulting from extended chains are aligned in one direction, one would then observe anisotropic behavior. (See Fig. 2.)

Therefore, if one could fully extend the chains and crystallize them in an oriented fashion one may be able to significantly improve uniaxially the tensile strengths and stiffness of the resulting films.

1.2 Theoretical and Experimental Stiffness of Extended Chains

Theoretical stiffnesses of fully extended chains have been calculated by Shimanouchi et al.[1]. Values for polyethylene and polytetrafluroethylene are shown in Table I and may be compared with observed values of these respective polymers which are randomly oriented. Polyethylene, for example, has been calculated to have a theoretical stiffness of 3.4×10^6 kg/cm^2, but the experimentally obtained stiffness is on the order of 10^3 kg/cm^2. The same orders of magnitude hold also for polytetrafluroethylene. Thus, the table points out that if one could fully extend the chains, one may realize an improvement in stiffness of three orders of magnitude.

1.3 Previous attempts to Prepare Chain Extended Crystals by Flow Induced Crystallization Systems

1.31 Mechanism of FIC

This method of producing chain extended crystals has been available since its discovery by Pennings[2] in 1960. Basically, Pennings took a solution of high density polyethylene (Marlex 50-Phillips) in xylene and isothermally sheared it between coaxial cylinders (See Fig. 3). Here, the inner cylinder may be rotated at any given velocity; however, at a certain critical velocity the flow pattern deviates from a simple shear flow to a secondary type of flow where Taylor

TABLE 1

THEORETICAL AND OBSERVED ELASTIC MODULI

POLYMER	THEORETICAL* $E_{11} \times 10^{-6}$ kg/cm^2	OBSERVED** $E \times 10^{-3}$ kg/cm^2
Polyethylene (High Density)	3.4	7.0
Polytetrafluoroethylene	1.6	4.2
Nylon		21.
PMMA		28.
Polypropylene		10.
DuPont Fiber B		170.

* T. Shimanovchi, et al., J. Polymer Sci., 59 93 (1962).

** M. Eisenstadt, Introduction to Mechanical Properties of Materials, MacMillan Co., New York, 1971.

vortices are formed. Pennings found these vortices to give the required tensile flow necessary for accelerated nucleation at high temperatures. Also, the fibrillar crystals were observed to deposit on the stirrer at the point where the fluid moves from the stirrer to the vessel wall[2].

Pennings further investigated the induction period for crystallization, which is the time elapsing between the beginning of stirring and the appearance of the first fibers. As may be seen in Figure 4, the induction time diminishes with increasing stirring speed according to the empirical relationship[2]:

$$\frac{1}{\tau} = \beta (n-15) \qquad (1)$$

where

τ = induction time in seconds

β = numerical constant depending on temperature

n = rpm of inner stirrer

From plots of $1/\tau$ vs n, one can obtain the minimum rate of stirring necessary, which for Penning's case turns out to be ~50 rpm.

How well this function of the induction time corresponds to the onset of secondary flow with Taylor vortices

can be seen by examining Table II. The minimum rate of stirring for the onset of Taylor vortices can be written in terms of a critical Reynolds number depending on the radius of the inner rotating cylinder, R, and ΔR, the annular gap between the inner and outer cylinders. One may then assess the critical speed, N_{CR}, by using this equation, where is the density and , the viscosity of the solution at the crystallization temperature. Equating (2) and (3), one obtains equation (4)--an expression for the minimum rate of stirring in terms of the vessel geometry. By inserting the appropriate values, Pennings[2] obtained 47 rpm which agrees remarkably well with the 50 rpm derived from eq. (1) from induction time data.

1.32 Morphology of FIC

Pennings[3] further studied the morphology of the resulting material produced by flow-induced crystallization. Figure 5 is a representation of the "shish-kabob" crystal structure exhibited in these experiments. It consists of a thin central thread of extended chain type which acts as a substrate for the transverse lamellar overgrowth of folded chains that form upon cooling to room temperature. The typical dimension of these "shish-kabobs" have been found

Table 2

	T_{cr} max. (^0C)	q (sec^{-1})	Re_{cr}	Flow-Pattern
No Stirring	96	-	-	-
Rotating outer cylinder	96	250	25,000	Laminar
Rotating inner cylinder	107	250	75	Taylor Vortices

$$Re_{cr} = 41.3 \quad \frac{R}{\Delta R}$$

$$Re_{cr} = \frac{2\pi \times N_{cr} \times R \times \Delta R \times \rho}{60 \times \eta}$$

$$N_{cr} = \frac{395 \times \nu}{\rho \; Rx(\Delta R)^3}$$

A. J. Pennings, Kolloid Z.u.Z. Polymere, 236, 99 (1970)

to be 100 Å x 200 Å for the width and thickness respectively of the central fiber 2100 Å for the diameter of the lamella spaced approximately 1100 Å apart. Furthermore, the average thickness of the lamella was seen to increase from 100 Å to 150 Å as the crystallization temperature increased.

1.33 Mechanical Properties of FIC

Stress-strain curves of the resulting material pulled parallel to the fiber axis were reported by Pennings[4]. All samples were produced from 5% solutions of Marlex high density polyethylene in xylene stirred at 500 rpm. The rate of testing was 3 cm/min on an Instron type tester. The results can be seen on Figure 6. It appears that at crystallization temperatures below 98°C the curves are representative of a soft, weak material whereas above 98°C, the curves take on the appearance of hard, brittle material. There is also much less extension at break, most likely due to better chain extension and more perfect crystals.

Examination of the tensile at break σ_b, vs crystallization temperature (Fig. 7) reveals much higher strength at higher crystallization temperatures and the reproducibility of the tensile strengths is better at lower T_c. Judging from this, the material seems more homogeneous at

lower T_c and may be due to the fact that crystallization proceeds at a relatively faster at low T_c, with the result being the inner cylinder is covered more uniformly than at higher T_c.

Finally, Pennings[4] correspondingly plotted the Young's Modulus vs. T_c (Fig. 8) and again the same effect is noted as in Figure 6. - higher stiffnesses but less uniformity at higher T_c. The maximum value here is about 17×10^4 kg/cm^2.

1.4 Previous Attempts to Prepare Chain Extended Crystals by High Pressure Systems

In a series of papers, Wunderlich[5,6,7] described the mechanism, morphology, and effect of pressure on the production of chain extended crystals under high pressures. Severely high pressures (upwards to 7 kBar) were found to be necessary since the samples were in the melt. Unfortunately the samples were too small to obtain specimens for examination of mechanical properties. However, this method allows an increase in crystallization temperature with increasing pressure--on the order of 2^0C/1000 psi.

1.5 Preparation of Highly Oriented Polymeric Films

The thrust of this project has been divided into two sets of experiments: (1) the influence of the shear rate on orientation/mechanical properties and (2) the effect of pressure at a given stirring rate on orientation/mechanical properties. A third set of experiments was contemplated utilizing increased T_c via pressure (Wunderlich) however time did not permit completion of these data.

For the above goals, a top stirred reaction vessel was constructed (Fig. 9) which permits pressurization (up to 5000 psi at 100^0 C) and stirring of solutions. The geometry of the cylindrical stirrer and annulus may be seen on Fig. 10.

1.6 Influence of Stirring Rate on Polyethylene Film Orientation

These films were studied by preparing a 3% solution of Marlex 6009 polyethylene ($\bar{M}_w$ = 169,000, $\bar{M}_n$ = 10,000) in xylene at 120^0 C. The hot solution was then poured into the reactor preheated to T_c (100^0 C in all cases). The solution was then stirred for 72 hrs at rates from 110 rpm to 380 rpm under atmospheric pressure. At the completion of the run the cylindrical stirrer was removed from the reactor and vacuum dried for 24 hrs. at T_c-2^0 C. The film was left on the stirrer during this time to preclude shrinkage. The film was then gently peeled from the stirrer and samples were then cut from it for testing.

1.61 Effect of Stirring Rate on Mechanical Properties of Polyethylene Films

Microdumbbells of the dimensions shown in Fig. 11 were cut from samples prepared as in 1.6. They were tested on a table model Instron using a cross-head rate of 5 cm/min. in the direction of orientation. The results are seen in Figs. 12 - 15.

As may be seen from the stress-strain curves, there is a trend of increasing modulus with stirring rate for these samples. However, the moduli and the stress at break were two orders of magnitude lower than those films prepared by Pennings at 100^0 C (see Fig. 7 and 8). The strain values for films prepared at 340 and 380 rpm were about the same as those shown on Fig. 7 and 8, i.e., less than 12%.

1.62 Effect of Stirring Rate on X-Ray Diffraction Patterns

Samples of films prepared in 1.6 were examined in a Phillips x-ray camera and wide angle x-ray diffraction patterns were taken. As may be seen in Figs. 16 - 19 no great amount of arcing is apparent as is expected of highly oriented crystalline polymers, although some arcing is seen. Stress direction is vertical in all patterns.

1.7 Influence of Pressure on Highly Oriented Polyethylene Films

The films in this set of experiments were prepared as follows: a 3% solution of Marlex 6009 HDPC in xylene was prepared

at 120° C. It was then poured into the preheated (100° C) reactor and pressure was then applied to the desired psi value. After stirring for 72 hrs at 225 rpm the cylindrical stirrer was removed and vacuum dried for 24 hrs at 98° C. The film was left on the stirrer during this period, again to preclude any shrinkage. The film was then gently peeled off the stirrer and samples cut from it for testing. Samples labeled 5, 10, 20, 30, 40, refer to 500, 1000, 2000, 3000, 4000 psi respectively.

1.71 Effect of Pressure on Mechanical Properties of Oriented Films

Samples dumbbells were cut from films produced in 1.7 and were tested on a table model Instron as in 1.61. The resulting stress strain curves are seen on Figs. 20 - 23 . The moduli and stress at break are again approximately two orders of magnitude lower than anticipated. Strain values appeared reasonable, i.e., less than 10%.

1.72 X-Ray Diffraction Patterns of Polyethylene Films

These wide angle x-ray diffraction patterns were taken using a Phillips x-ray camera and are seen on Figs. 24 - 27 . Stress direction vertical in all cases. Again, no great deal of arcing is seen in the samples.

1.73 Effect of Pressure on DSC of Polyethylene Films

DSC measurements were taken on these films using a Perkin-Elmer DSC. The scan rate was 5° C/min in all cases. Melting

points and heat capacity were referenced to standard tin samples. Calculations of percent crystallinity were calculated by areas under the melting curve. These are seen on Figs. 28-31.

One notes that melting points and percent crystallinity are not much greater than that of a commercial polyethylene, i.e., 135^0 C and 549 respectively.

1.8 Summary of Oriented Films Produced under Shear and Pressure

As may be seen, the moduli, stress at break, X-ray and DSC point out no great amounts of orientation from films produced as in sections 1.6 and 1.7. There does seem to be trends of higher orientation with increasing shear, but lower orientation with increased pressure. See Fig. 32a,32b. Two probable causes are that the reactor should be preheated to 120^0 C (same temperature as the prepared solution) and then brought down T_c, and that the pressure may reduce the free volume of the polymer in solution. If this latter effect does take place, it means increased rates of crystallization and less freedom of chain mobility to achieve high orientation.

Screening of Polymers for Early Oriented Extended Chain Crystals

2.0 Introduction

While itwas known that polyethylene and polyethylene oxide did form extended chain crystals under shear or high pressure, it was not known if other more rigid polymers might be crystallized in an extended form under less drastic conditions. Therefore it was proposed in the contract that more rigid-like polymers be examined to see if extended and oriented chain crystal could be formed.

It seemed appropriate to see if polymers could be crystallized in chain extended film using only a small amount of material. For screening purposes it was necessary to use small amounts of material if new polymers were to be examined. One technique of imposing order on a polymer film is to make the thickness so small that the substrate imposes an order on the polymer molecules as the solvent evaporates[8,9,10]. This involves small amounts of material (film thicknesses of ~1000 Å).

Another method to obtain extended chain crystals in films is through the extrusion of rigid molecules[11,12]. For screening purposes this could be accomplished with small amounts of material by working with very stiff materials that could orient with only their own viscous drag while being pulled out of the melt.

Finally it seemed reasonable to see if a crystalline polymer domain surrounded by a rubber matrix would have any orientation if

the crystallization took place under the tensile forces of the surrounding elastomeric molecules. In particular oriented films of small thickness ($\sim$1000 $\mathring{A}$) could be obtained by working near the stoichiometry required for sheet-like domains.

3.0 Ultra-thin Film Casting

It was decided that ultra-thin film casting might be an effective screening method for determining quickly whether oriented structures could be formed. Three classes of material were selected for the preliminary screening: i) a flexible polymer(polystyrene), ii) a semi-stiff polymer(cellulose acetate) and iii) a rigid polymer(polyalkyl-isocyanates). (See Table III).

The first class of polymers is like those of polyethylene and polyethylene oxide in having a rather flexible chain backbone. However the polystyrene was atactic and couldn't crystallize so that the attempt was to examine the effect of ultra-thin casting on non-crystalline ordering. The cellulose acetate does crystallize and can give rather strong crystalline peaks although there is still some amorphous material. The poly-alkyl-isocyanates are known to be rigid rods[13]. These materials are highly crystalline and would be expected to form an ordered liquid structure under even a small shear gradient. These materials are like polypeptides in that they are known to be helix forming even in solution.

Table 3
Polymeric Classes Scheduled for Screening

i) 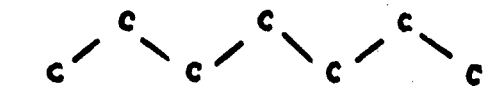

polyethylene

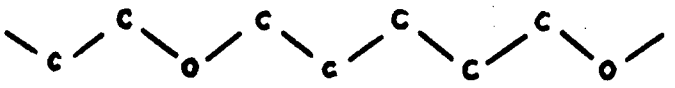

polyethylene oxide

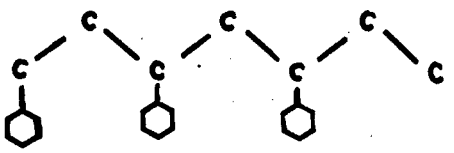

polystyrene

ii) 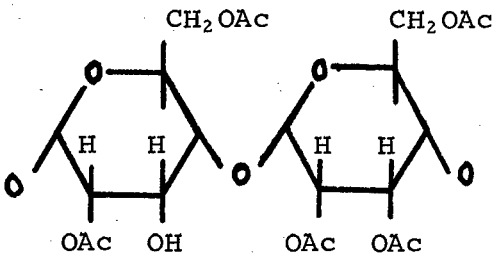

cellulose acetate

iii) 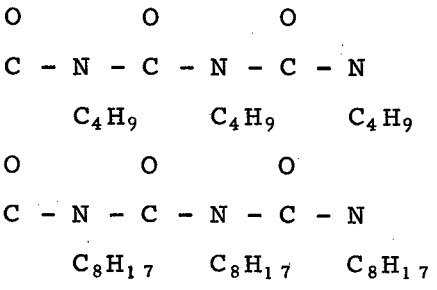

polybutylisocyanate (PBIC)

polyoctylisocyanate (POIC)

If larger amounts of such rigid polymeric material could be obtained, they should have great promise of chain extension when the stirred, high pressure reactor is used for the crystallization.

3.1 Polystyrene

Figure 33 shows that ultra-thin films cast from an amorphous polymer exhibit little significant mechanical difference when examined either parallel or perpendicular to the casting direction or when compared to thick films.

3.2 Cellulose Acetate

Figures 34 and 35 indicate that the ultra-thin films cast from cellulose acetate also do not show any significant difference in mechanical properties when examined parallel or perpendicular to the casting direction, or when compared to thick films.

3.3 Poly(n-alkylisocyanates)

Ultra-thin films of poly n-butyl isocyanate (PBIC) were cast from dilute benzene solutions using a glass-plate dipping technique. The equipment used was 2 x 10 inch glass plates, a tall container for the polymer solution and a drive mechanism to introduce and withdraw the glass plates from the solution. The whole assembly is shown in Fig. 36[8]. The thickness of the films obtained is in the order of 250 $\mathring{A}$. Three hundred layers of these ultra-thin films were stacked together and examined by stress-strain measurements. A comparison of the results to that of the films of 0.05 mm.

thickness cast by conventional techniques is shown in Fig. 37 . It indicates that the thin films have very few different mechanical properties. That is, the ultimate breaking strengths of the ultra-thin films are initially larger than those of the thick films.

The initial moduli have not been determined with sufficient precision to determine if there is a significant difference between the two types of films.

X-ray flat plate pictures for ultra-thin and thick films of PBIC are shown in Figs. 38 and 39. Since the poly (n-alkyl isocyanate) molecules exist as rigid rods in solution, it was thought that by thin film casting these molecules should crystallize as extended chains and orient in the spreading direction. Unfortunately, from the X-ray pictures it is seen that no preferred orientation exists in either ultra-thin films or thick films. The corresponding Bragg's spacings are listed in Table IV.

3.4 Benzyl-L-Glutamate

Samples purchased from Sigma Chemical Corporation were dissolved in chloroform and cast as thick films and ultra-thin films. X-ray analysis using a flat-plate camera shows in Fig. 40 some arcing but not enough to consider any significant ordering. Other scientists have found significant orientation of this material when the casting solution is subject to an electric field. Stretching the fiber afterward did not appreciably improve the orientation due to the onset of failure. Optical microscopy indicates a liquid-crystal orientation of the rod-like structures, as reported earlier

Table 4

Observed Bragg's Spacings for Ultra-thin and Thick Films of PBIC

Ultra-thin Film	Thick Film
11.37	11.74
	7.31
6.93	5.89
4.85	4.91
4.10	4.55
3.86	4.15
	3.79
3.07	3.40
2.84	3.07
2.50	2.84
	2.57
2.29	

by Banford

It was hoped that even more extended rigid polymers like the polybenzimidazoles or Kevlar could be handled in this form for screening. Unfortunately none of the latter materials showed any significant promise when prepared by the ultra-thin film casting techniques.

4.0 Melt Oriented Polymers

Rigid polymers ought to be easily oriented by extrusion from the melt. Therefore films pulled from the melt of rigid polymers should contain extended crystals. In order to test this hypothesis three rigid chain polymers were studied: poly n-alkyl isocyanates, poly- -benzyl l-glutamate, and Kevlar.

4.1 Poly (n-alkyl isocyanates)

First there was a need to know more about the structures of n-alkyl isocyanate polymers. For this purpose x-ray diffraction studies were made of samples prepared in the bulk state. The melting point is very close to the temperature at which chain degradation begins so that care must be taken not to destroy the small research samples that were given to the grant through the generosity of Professor L. J. Fetters of the Institute of Polymer Science. The molten sample under no external stress showed no orientation. However, the sample pulled from the melt on a pin and subject only to the internal stress of its own viscous forces did show orientation.

Oriented specimens of poly(n-alkyl isocyanates) were obtained by simple viscous drawing from the polymer melts. A typical X-ray fiber pattern for PBIC is shown in Fig. 41a. The equatorial arcings are an indication that the polymer chains have preferentially aligned themselves in the fiber axis. For comparison, Fig. 41b shows an X-ray picture of a randomly oriented PBIC sample. The corresponding Bragg's spacings for both samples are listed in Table V. These spacings are in approximate agreement with the data obtained by Shmueli, Traub and Rosenheck[12] . The structure they deduced is a hexagonal packing of the polymer molecules with unit cell parameters a = 13.3 $\mathring{A}$ and, c = 15.5 $\mathring{A}$, respectively. An electron diffraction pattern taken from this sample confirms the hexagonal packing as shown in Fig. 42 .

Since n-butyl isocyanate structures do show a clear chain folding tendency at high molecular weight, it was of interest to see if the reason for the lack of clear orientation was the folding of the chains. (The available samples were all high molecular weight whole polymers.) Figure 43 and Figure 44 show both the X-ray and thermal analytical (DSC) traces of possible transactions in these polymers. There is a reversible transition in PBIC at 70° high molecular weight material. Low molecular weight samples do not have this transition. Consequently the problem in orientation may come from the high molecular weight sample. Unfortunately

Table 5

Observed Bragg's Spacings for Poly(n-butyl Isocyanate), Å

Oriented Sample	Unoriented Sample
20.52 (E)*	
	10.94
10.31 (E)	
	4.85
	4.29
7.22 (E)	3.94
	3.02
6.55 (E)	2.98
	2.86
4.85 (M)	2.68
	2.46
4.29 (M)	2.31
	2.03
3.02 (M)	1.89

*E: Equatorial

M: Meridional

X-ray studies of the same high molecular weight polymer (PBIC) show the emergence of a strong crystalline peak nera 14^0. This 6.4 $\overset{0}{A}$ spacing is annealed in and is not reversible. However, only low angle x-ray scattering could be expected to show the disappearance of a long fold spacing. Therefore the DSC results are probably indicative of a chain motion that can lead to better crystals or possibly chain folds.

Poly n-hexyl isocyanate (PHIC)

With only a small amount of PHIC available, it was necessary to use a concentrated solution rather than the melt because some degradation at the melting temperature could occur. A concentrated PBIC solution (60%) in chloroform was therefore made and a fiber and also film were withdrawn from the viscous solution. Figure 45 shows the orientation of both fiber and film. Table VI gives the pertinent spacings. This material would be exceptionally good for the prepared studies it it were available in 100 g quantities.

Table 6

PHIC

Bragg's Spacings of Oriented PHIC Films and Fibers* (Å)

Equatorial	Meridional	Near Meridional
15.46		
10.86		
9.23		
8.04		
6.48		
5.35		
		4.72
4.68		
	4.05	
	3.66	
		3.35
	2.96	
		2.73
	2.57	
		2.22
	1.93	
	1.86	

*The degree of orientation and Bragg's Spacing for the films and fibers are the same.

Figure 46 shows an X-ray fiber pattern for poly (n-octyl isocyanate)(POIC). The random orientation pattern is shown in Figure 47 . As can be seen, the replacement of the butyl side chain by octyl group does not change the crystal structure to any extent. The corresponding Bragg's spacings are listed in Table VI.

Table 7

Observed Bragg's Spacings for Poly(n-Octyl Isocyanate), Å

Oriented Sample	Unoriented Sample
19.33 (E)	19.33
16.44 (E)	16.44
14.32 (E)	
10.94 (E)	10.94
10.31 (E)	
7.22 (E)	7.22
6.25 (E)	6.25
6.19 (E)	
4.85 (M)	4.85
	4.55
4.29 (M)	4.29
3.02 (M)	3.02
2.93 (M)	2.93
	2.57

5.0 Kevlar

A new type or organic synthetic fiber having specific tensile moduli greater than twice that of E-glass fibers has been developed recently. It is commercially available from the E. I. Du Pont Co. as Kevlar fibers. The chemical formulas for these types of polymers are either 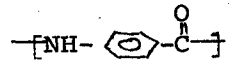 or 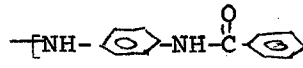 . Monsanto also developed similar types of polymers with the following formulas; 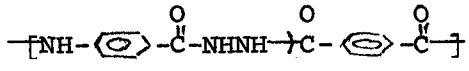 and 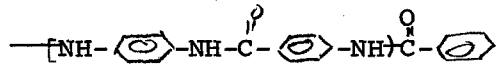 .[6]

Highly oriented film from these types of polymers seemed useful for this research. Therefore requests of the above companies were made for the above resins. Unfortunately the only material received was from the E.I. DuPont Co. and consisted of already spun Kevlar fibers Due to their para-oriented aromatic characteristics these fibers possess high melting points and are extremely difficult to remelt and avoid thermal degradation. In addition no common organic solvents redissolve these fibers so that a polymer film can be easily cast from the solution.

These fibers were therefore dissolved in inorganic solvents. The only successful solvent was concentrated sulfuric acid, although difficulties were encountered in casting films from this solvent. DMSO did not dissolve the material.

Solution preparation: Reagent grade concentrated sulfuric acid was used as a solvent. It contained at least 95% H_2SO_4. The Kevlar fibers were cut in short length and separated from the bundle to increase the contact surface with H_2SO_4. An erlenmeyer flask with a ground joint was filled with concentrated H_2SO_4 and then the cut fibers were put in and stirred with a magnetic stirring bar. To prevent the absorption of moisture from the atmosphere, the flask was capped with a ground joint top. A 50% solution can be prepared within 24 hrs.

Film casting: The Kevlar films were prepared by pouring the concentrated H_2SO_4 polymer solution onto a glass plate and then spreading the viscous solution with a glass slide. The glass plate was then immersed in a bath filled with running water. The polymer film was then easily separated from the glass plate after the sulfuric acid was washed away. To insure the complete removal of the acid, the polymer films were kept in the water bath for 3 hours. Then a plastic straw was used to roll up the polymer films which were later put in an oven at 110^0 C to dry 2 hours. Another method used to remove the residual acid was through the addition of NaOH to neutralize the acid. A failure to remove completely the H_2SO_4

causes scorching of the film. The final dry films for X-ray analysis were obtained by slitting the straws.

X-ray diffraction: The X-ray flat plate method was used to study the nature of crystallinity of the cast films. Figure 48 shows a picture taken from the original cast film. The diffuse halo indicates that there is not much crystallinity in the as-cast film. When this film was put under an optical microscope, a lot of air bubbles can be seen. These air bubbles were formed when the concentrated H_2SO_4 polymer film was first put in contact with water and subsequently heated. Ice-water was used to try to minimize the heating, but with very little success. The presence of air bubbles seems to be the major problem.

Annealing with super-heated steam was employed to increase the crystallinity of the film. Figure 49 shows the X-ray flat plate picture of an annealed film. It is seen that the degree of crystallinity was increased somewhat. Although stress was applied to the film in the hope of getting the preferred orientation, which exists in the original Kevlar fiber (figure 48), it does not reappear in the cast films. However the Bragg spacings are equivalent. It is likely that the lack of orientation is due to the brittleness of the film that allow very little stretching.

Stress-strain measurements: A table model Instron Tester was used to measure the tensile strength and modulus. Of the samples tested, the average strain at break was about 3% and the stress at break was 1.4×10^3 kg/cm^2. The stress-strain response was linear up to the break point. No yielding was observed. The Young's modulus was to be $E_{11} = 3.7 \times 10^4$ kg/cm^2.

References

1. T. Shimanouchi, M. Asahini, and S. Enomoto, J. Polymer Sci., 59, 93 (1942).

2. A. J. Pennings, J. Phys. Chem., Solids Supplement, No. 1, 389 (1967).

3. A. J. Pennings, J. Van der Mark, and A. Kiel, Kolloid Z.u.Z. Polymere, 237 (2), 336 (1970).

4. A. J. Pennings, J. Van der Mark, and H. Booy, Kolloid Z.u.Z. Polymere, 236 (2) 99 (1970).

5. B. Wunderlich, J. Polymer Sci., A 3697 (1964).

6. B. Wunderlich, T. Davidson, J. Polymer Sci., A-2, 2043 (1969).

7. B. Wunderlich, Pure and Applied Chem., 31, 49 (1972).

8. S. Krishnamurthy and D. McIntyre, Reverse Osmosis Membrane Research, ed. H. K. Lonsdale and H. E. Podall, Plenum Press New York, 1972, p. 457.

9. S. Krishnamurthy and D. McIntyre, Polymer Letters, 10 647 (1972).

10. S. Krishnamurthy, D. McIntyre, E. R. Santee, Jr., and C. Wilson, J. Polymer Sci., (Phys.) 11, 427 (1973).

11. W. Burchard, Makromol. Chem. 67, 182 (1963).

12. U. Shmueli, W. Traub and K. Rosenheck, J. Polymer Sci., A-2, 7, 515 (1969).

13. W. B. Black and J. Preston, Eds., "High Modulus Highly Aromatic Films", M. Dekker, N. Y., 1973.

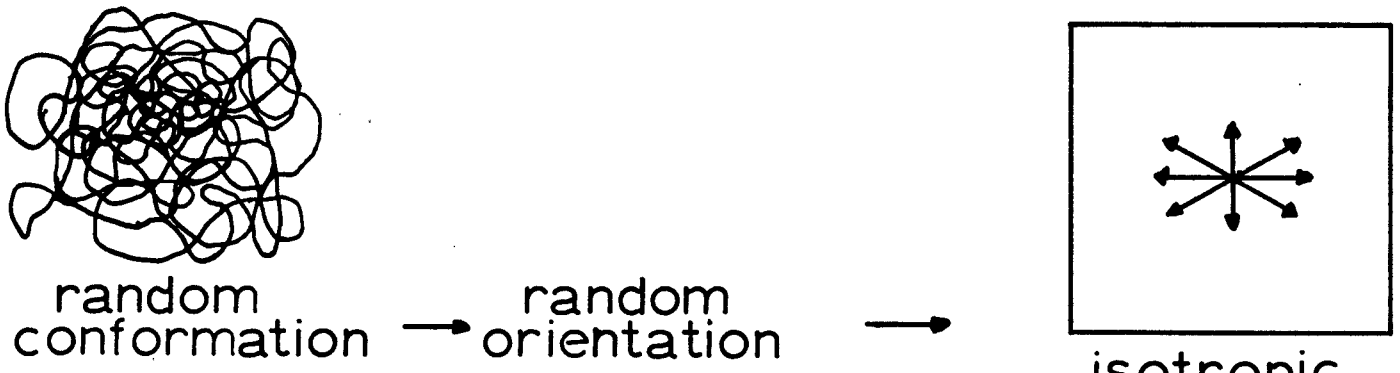

Figure 1. Random Chain Conformation and Isotropicity

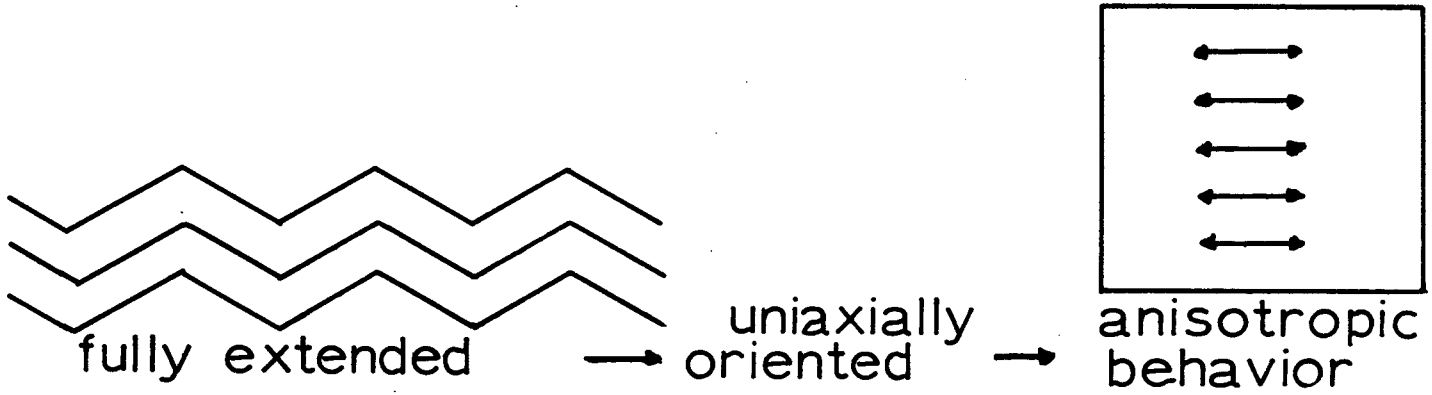

Figure 2. Uniaxial Chain Extension and Anisotropicity

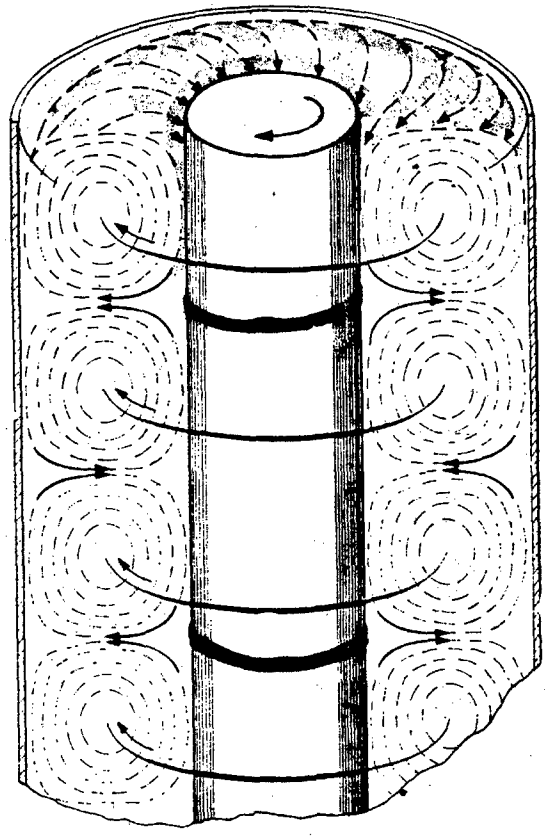

Figure 3
Cross Section of Coaxial Cylinders
Under Crystallization Conditions

A. J. Pennings, Kolloid .Z.u.Z. Polymere
236, 99, (1970)

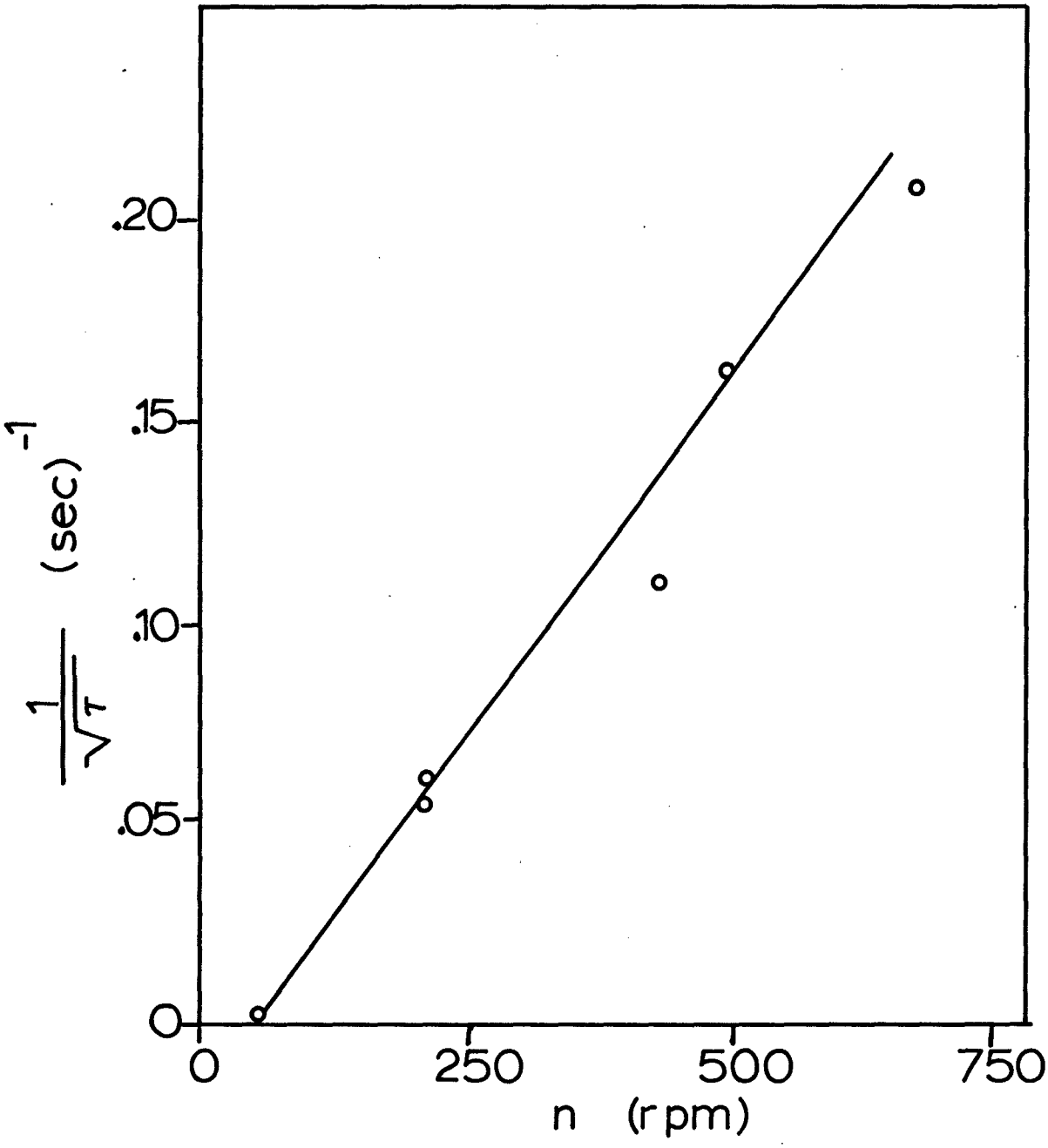

$$\frac{1}{\sqrt{\tau}} = \beta(n-15)$$

Figure 4. Effect of Stirring Rate on Crystallization Induction Times

A. J. Pennings, Kolloid-Z.u.Z. Polymere, 236 99, (1970).

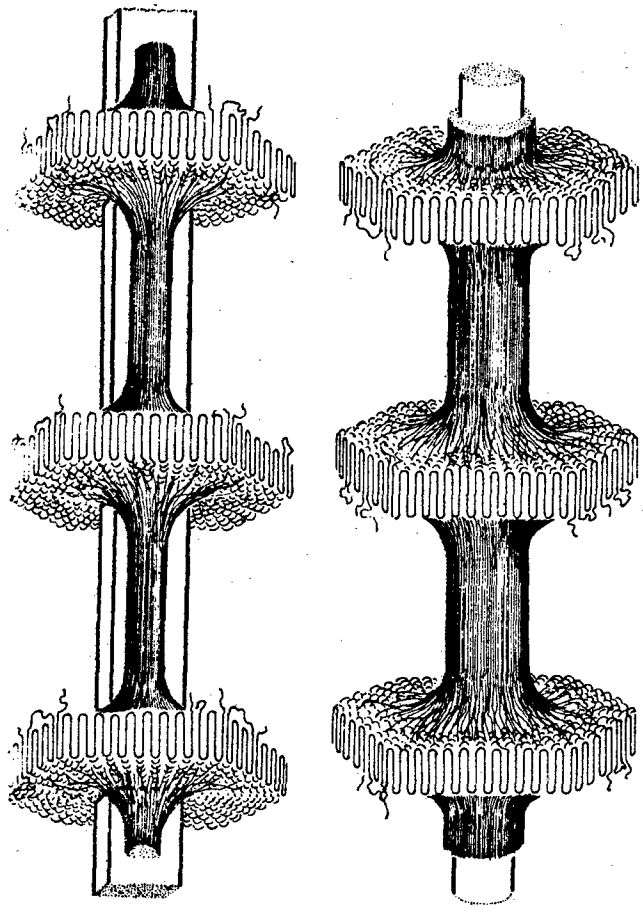

Figure 5

Morphological Models of Crystallization Induced Orientation of Polymer Molecules

A. J. Pennings, Kolloid Z.u. Z. Polymere, 237, 336, (1970)

Figure 6

Stress Strain Curves of Polyethylene Films Obtained from Stirred Solutions

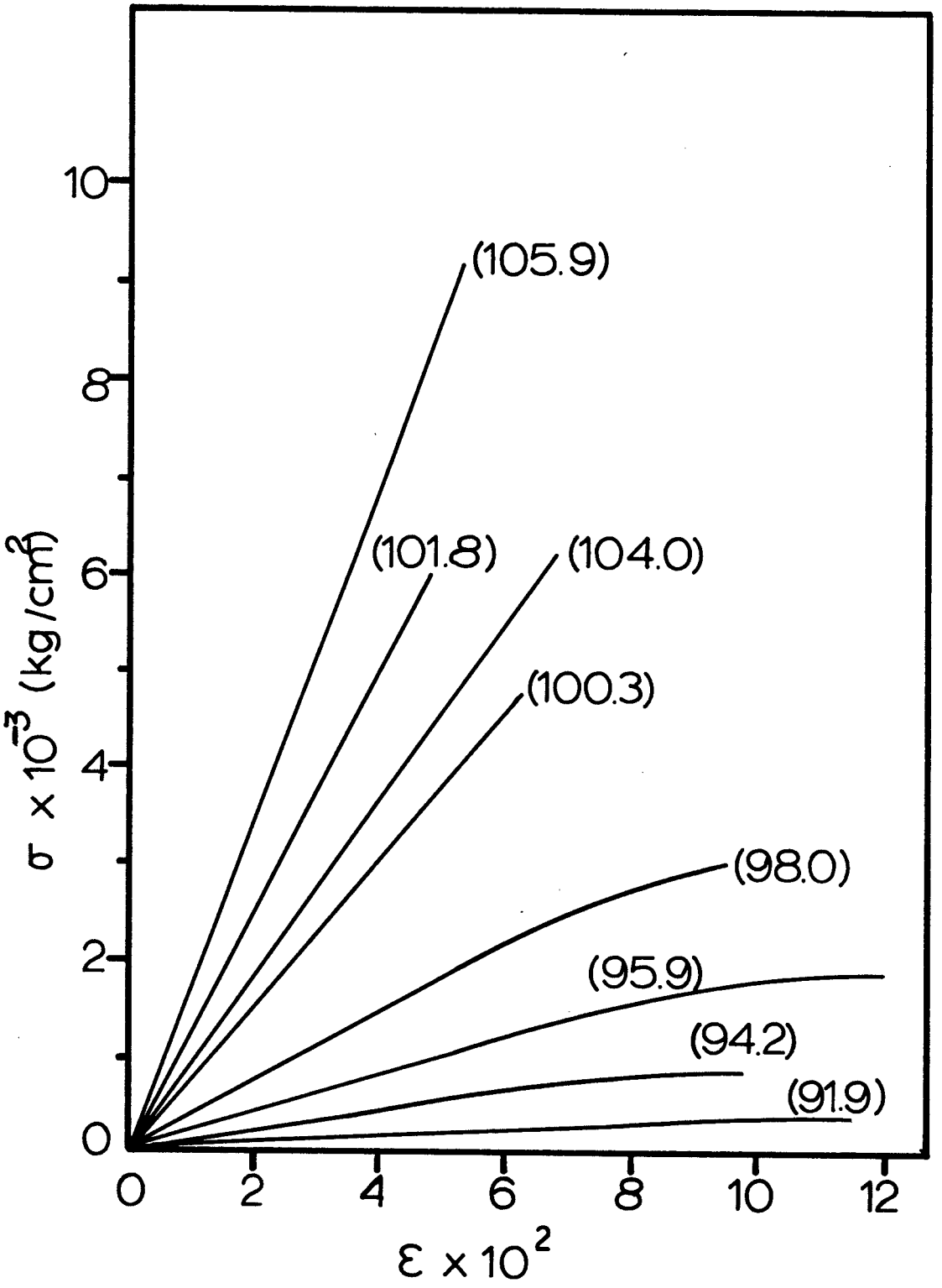

A. J. Pennings, J. Polym. Sci., C, 38, 167, (1972)

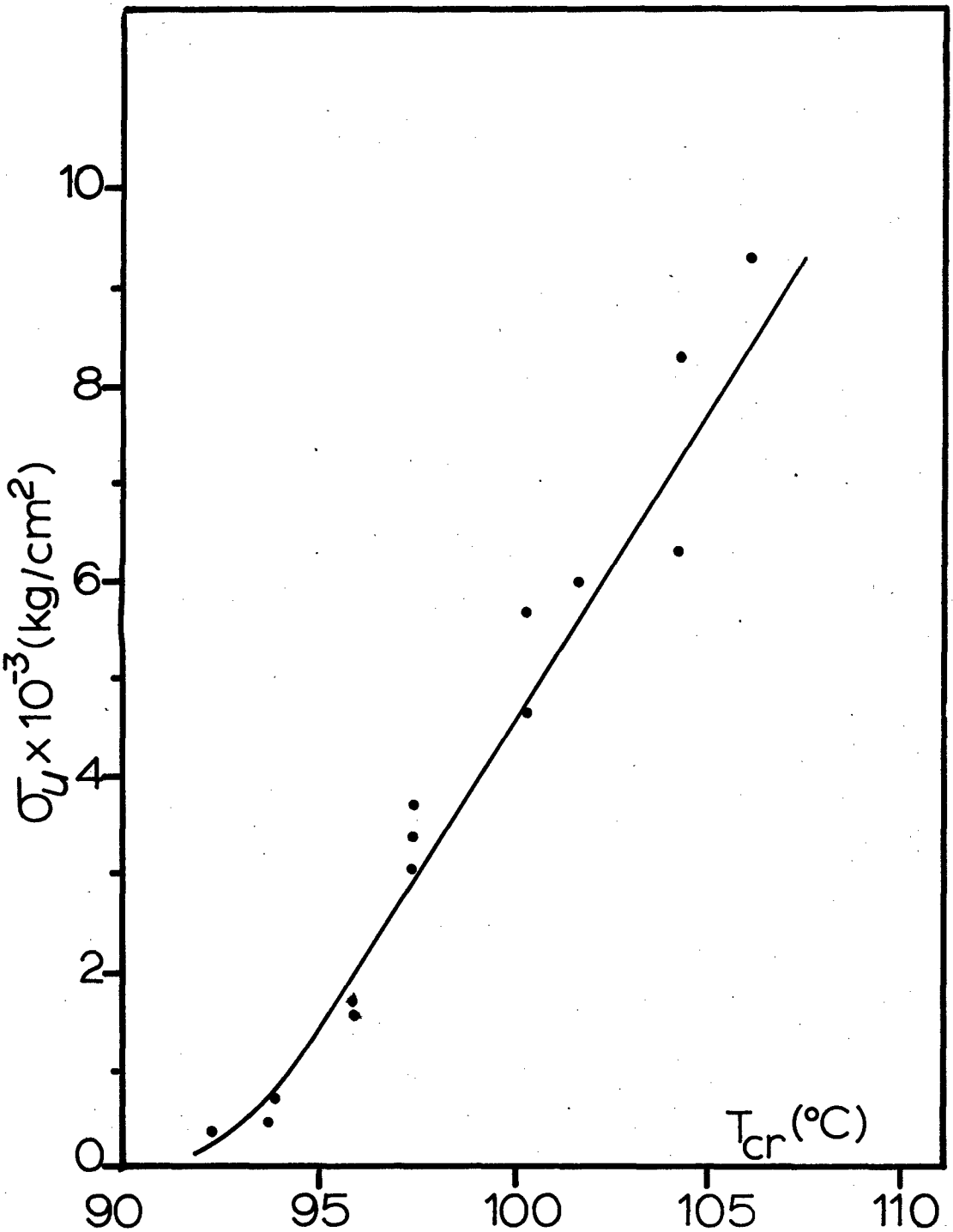

Figure 7. Stress at Break, , vs. T_c for Polyethylene Films Obtained from Stirred Solutions.

A. J. Pennings, J. Polym. Sci., C, 38, 167, (1972)

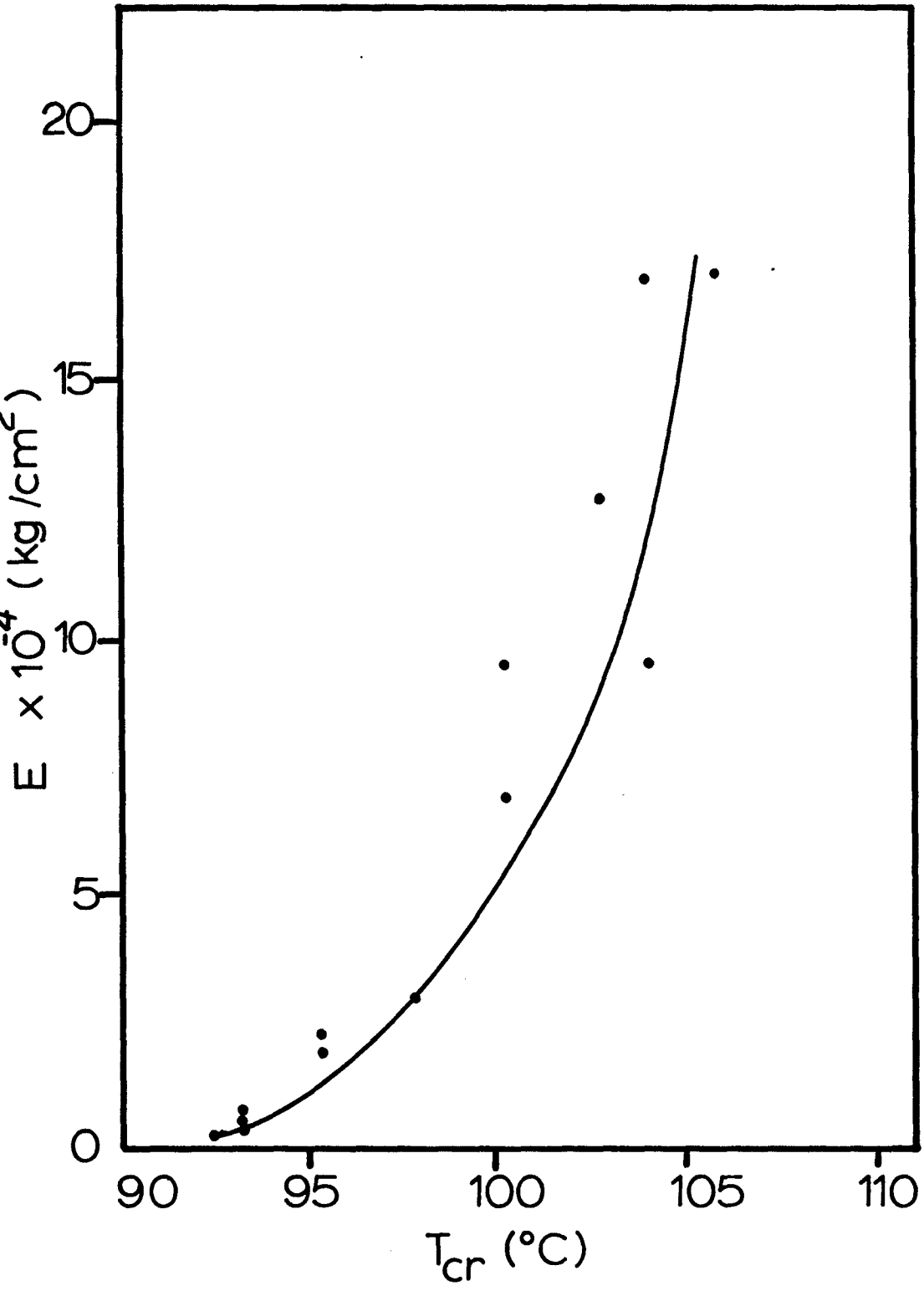

A.J. Pennings, J. Polym. Sci., C, 38, 167, (1972)

Figure 8. Modulus vs. T_c for Polyethylene Films Obtained from Stirred Solutions.

Figure 9

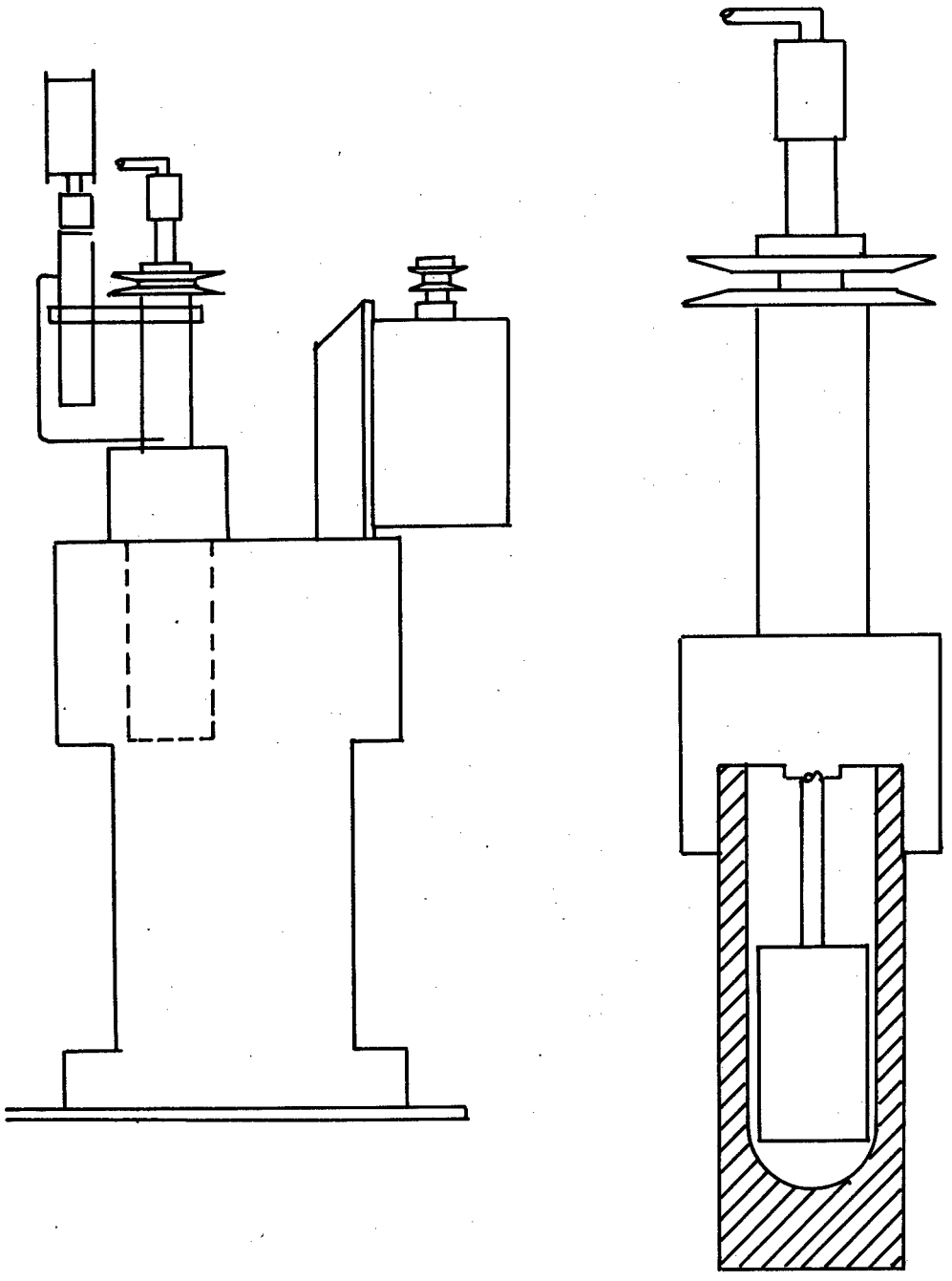

Pressurizable Coaxial Cylinder Stirring Apparatus

Figure 10

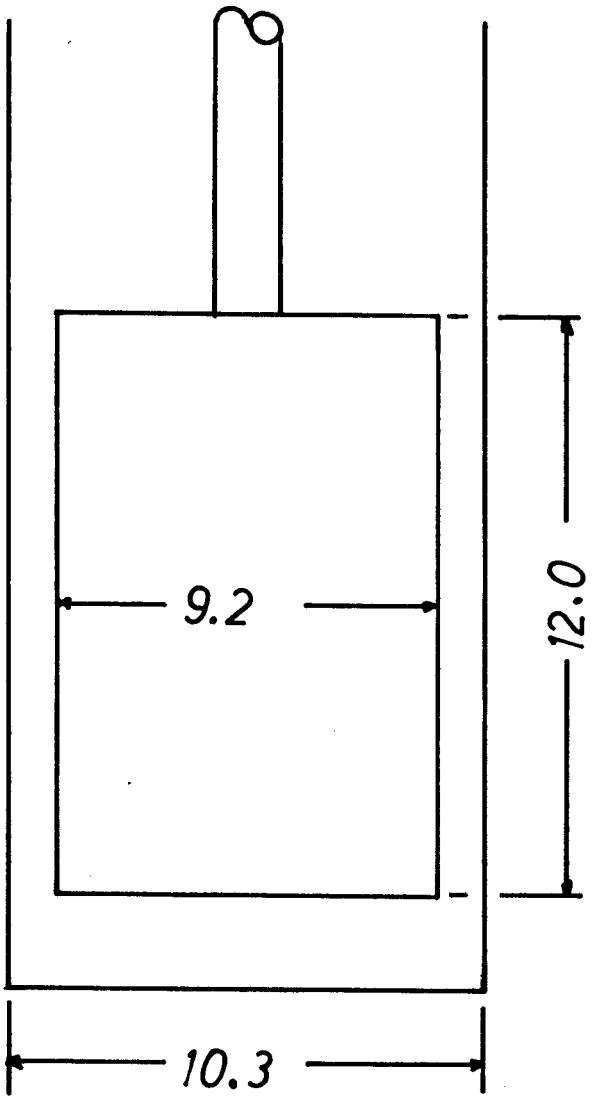

STIRRER GEOMETRY IN CM.

Figure 11

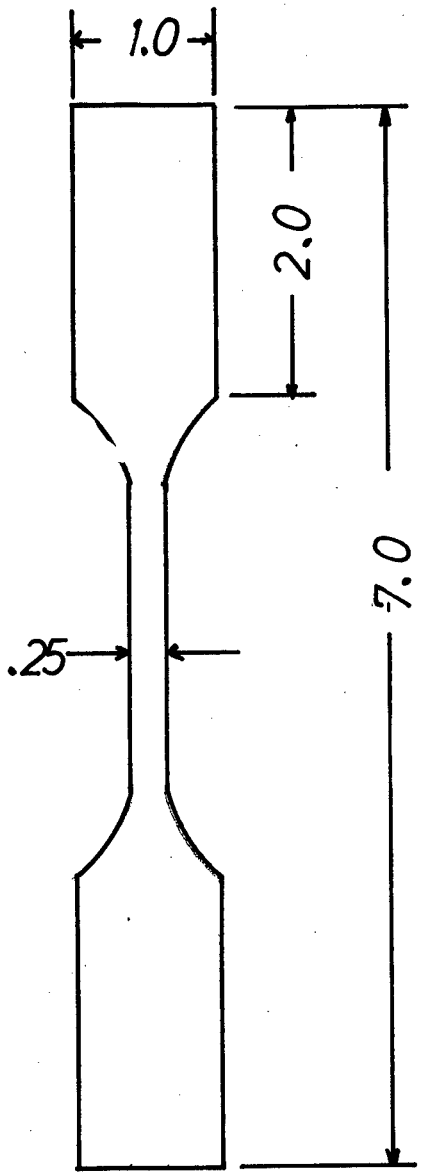

MICRODUMBELL GEOMETRY
IN CM.

Figure 12

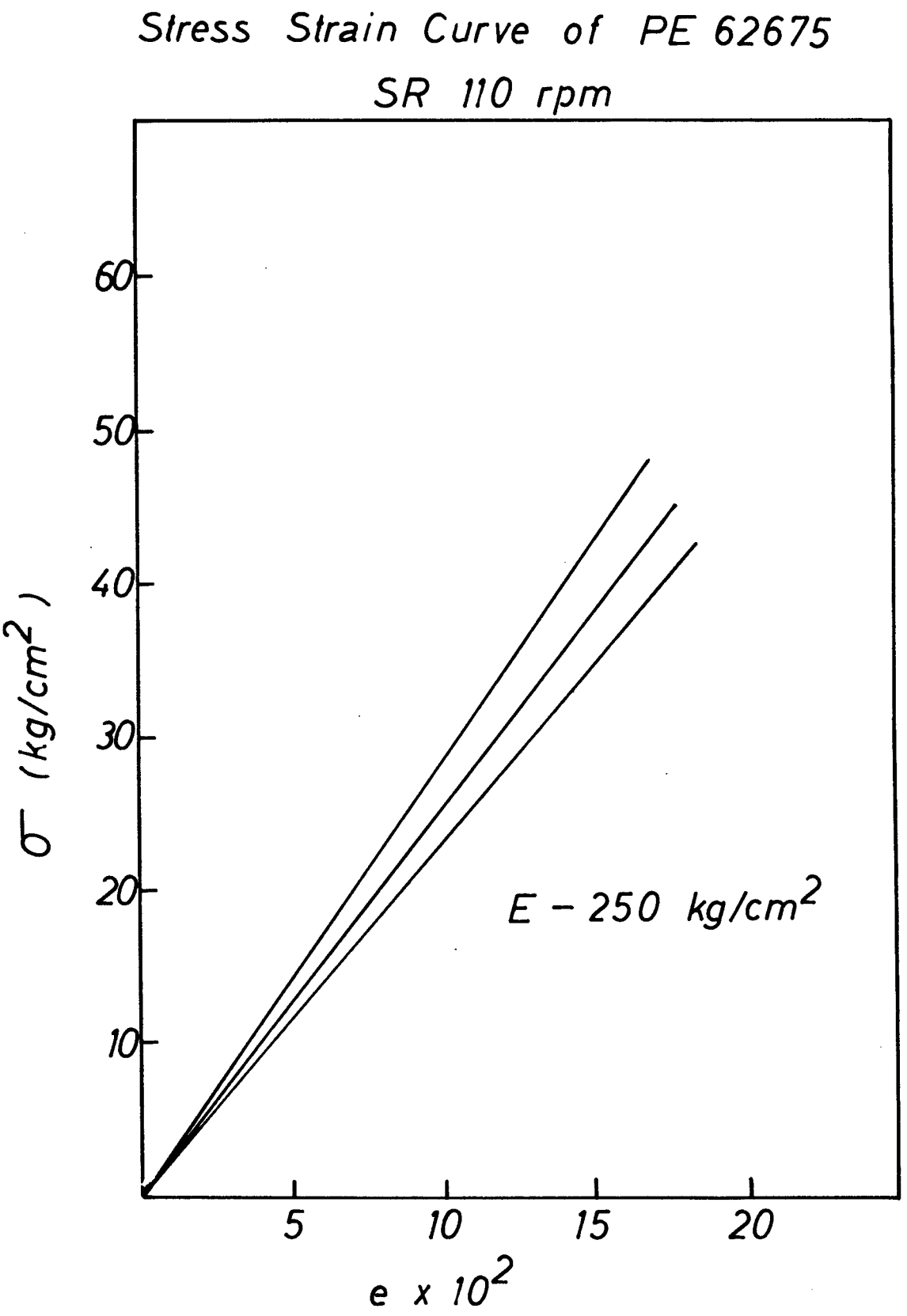
Stress Strain Curve of PE 62675
SR 110 rpm
60
50
40
30
20
10
σ (kg/cm²)
E - 250 kg/cm²
5
10
15
20
e x 10²

Figure 13

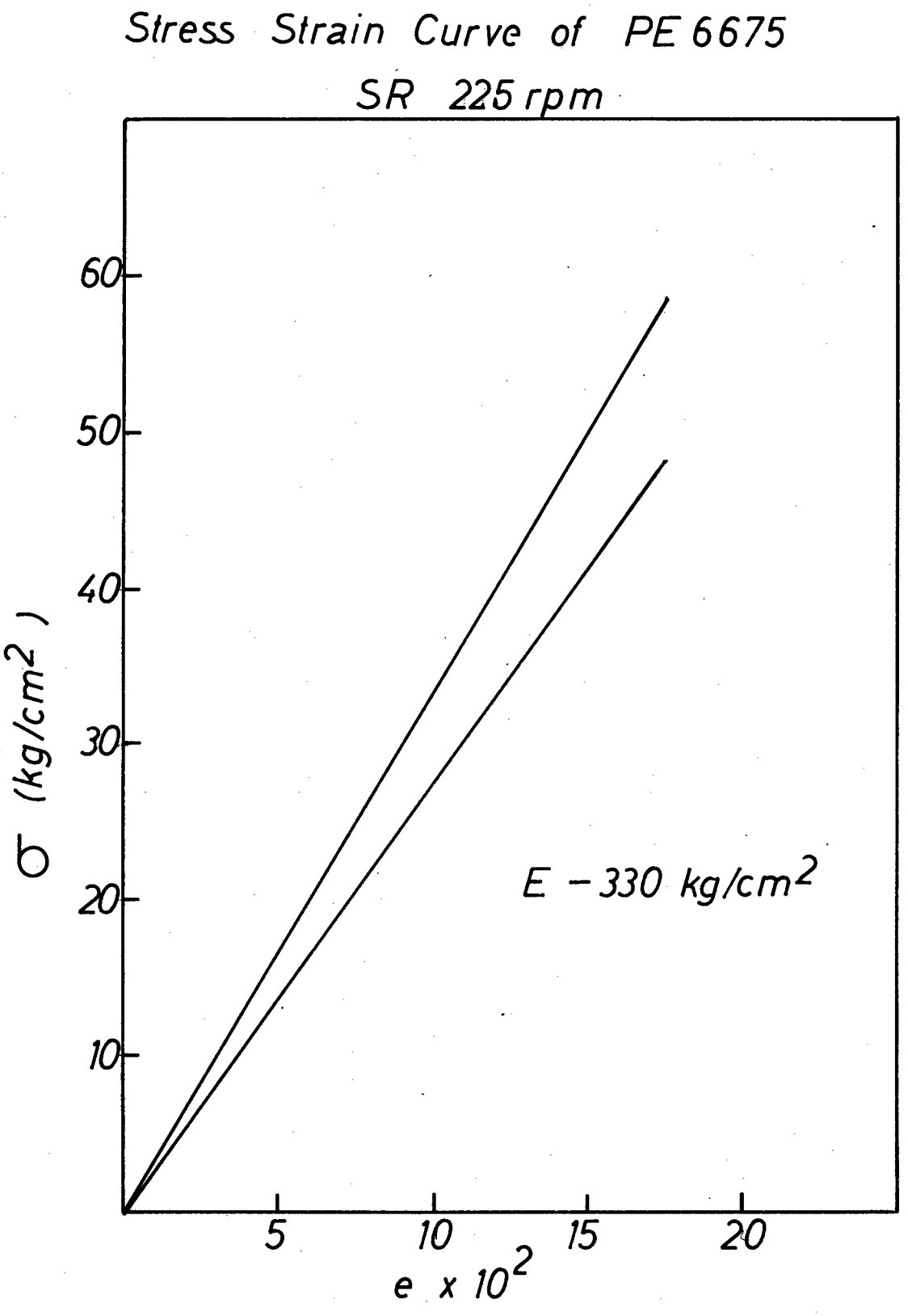
Stress Strain Curve of PE 6675
SR 225 rpm
60
50
40
30
20
10
σ (kg/cm²)
E - 330 kg/cm²
5
10
15
20
e x 10²

Figure 14

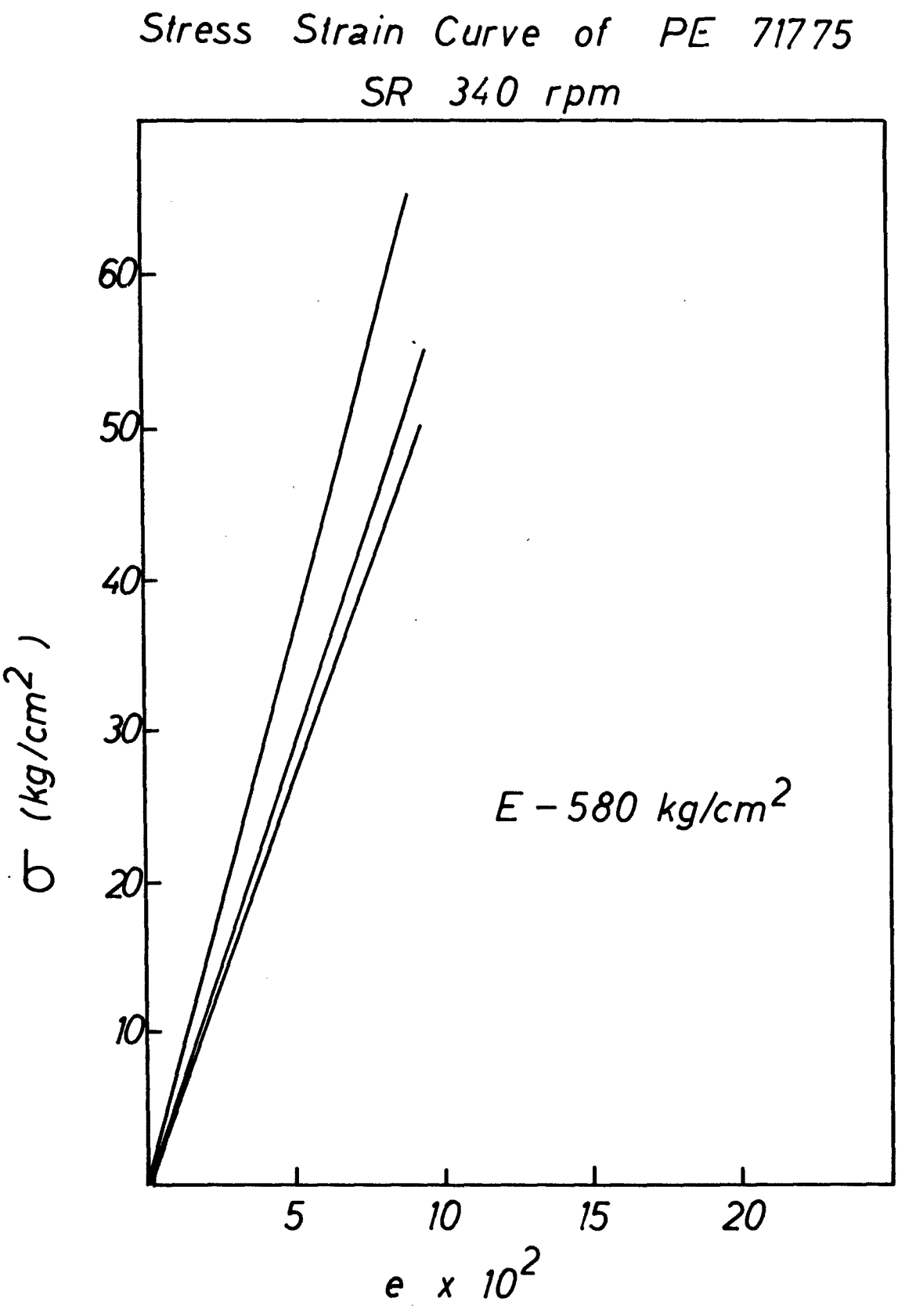
Stress Strain Curve of PE 71775
SR 340 rpm
60
50
40
30
20
10
σ (kg/cm²)
E - 580 kg/cm²
5
10
15
20
e x 10²

Figure 15

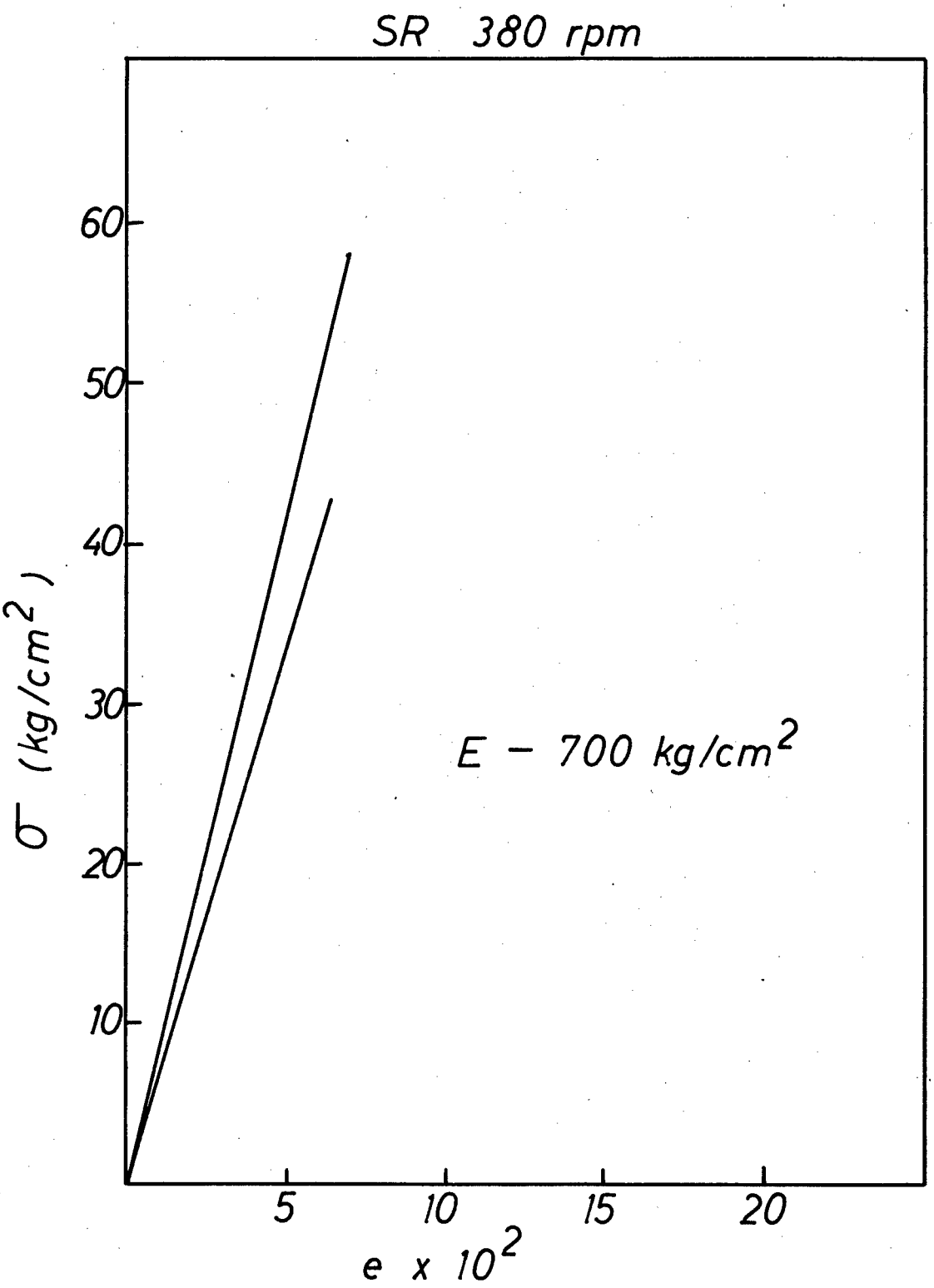

Stress Strain Curve of PE 7175

Figure 16

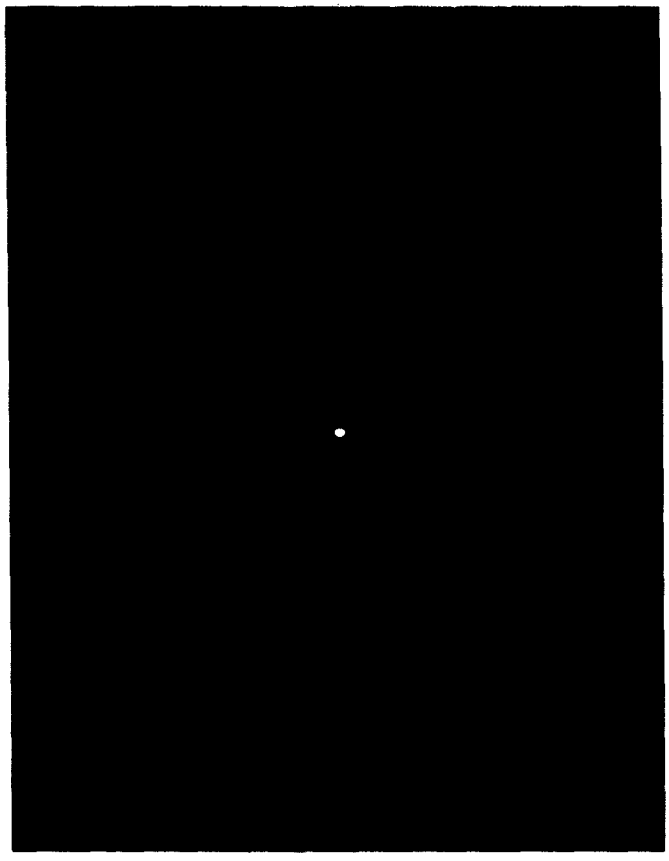

Wide Angle X-Ray Diffraction Pattern of PE

(110 rpm)

Figure 17

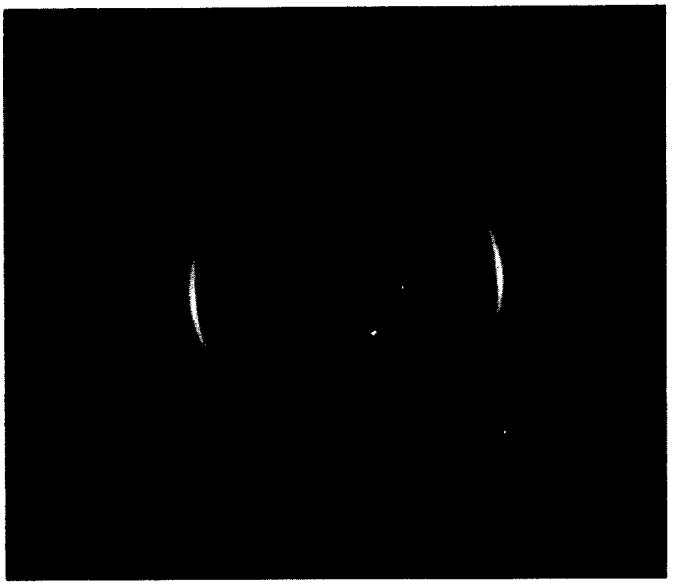

Wide Angle X-Ray Diffraction Pattern of PE

(225 rpm)

Figure 18

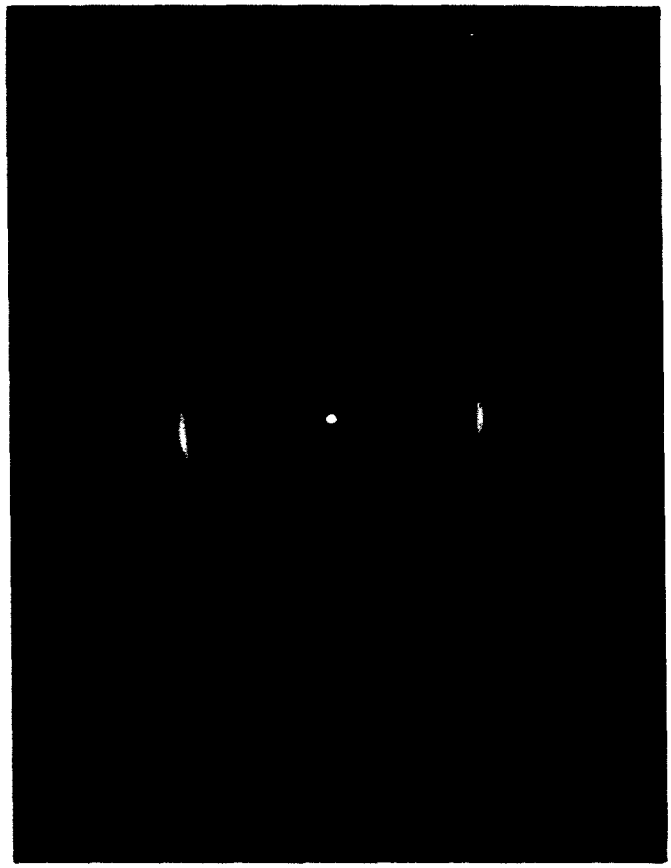

Wide Angle X-Ray Diffraction Pattern of PE

(340 rpm)

Figure 19

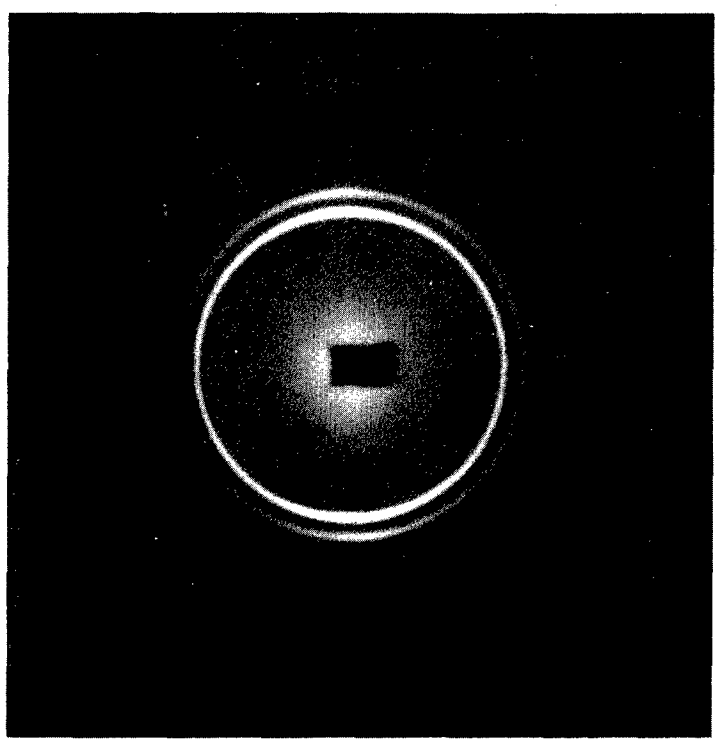

Wide Angle X-Ray Diffraction Pattern of PE

(380 rpm)

Figure 20

Stress Strain Curve of PE 102074

P-500 psi

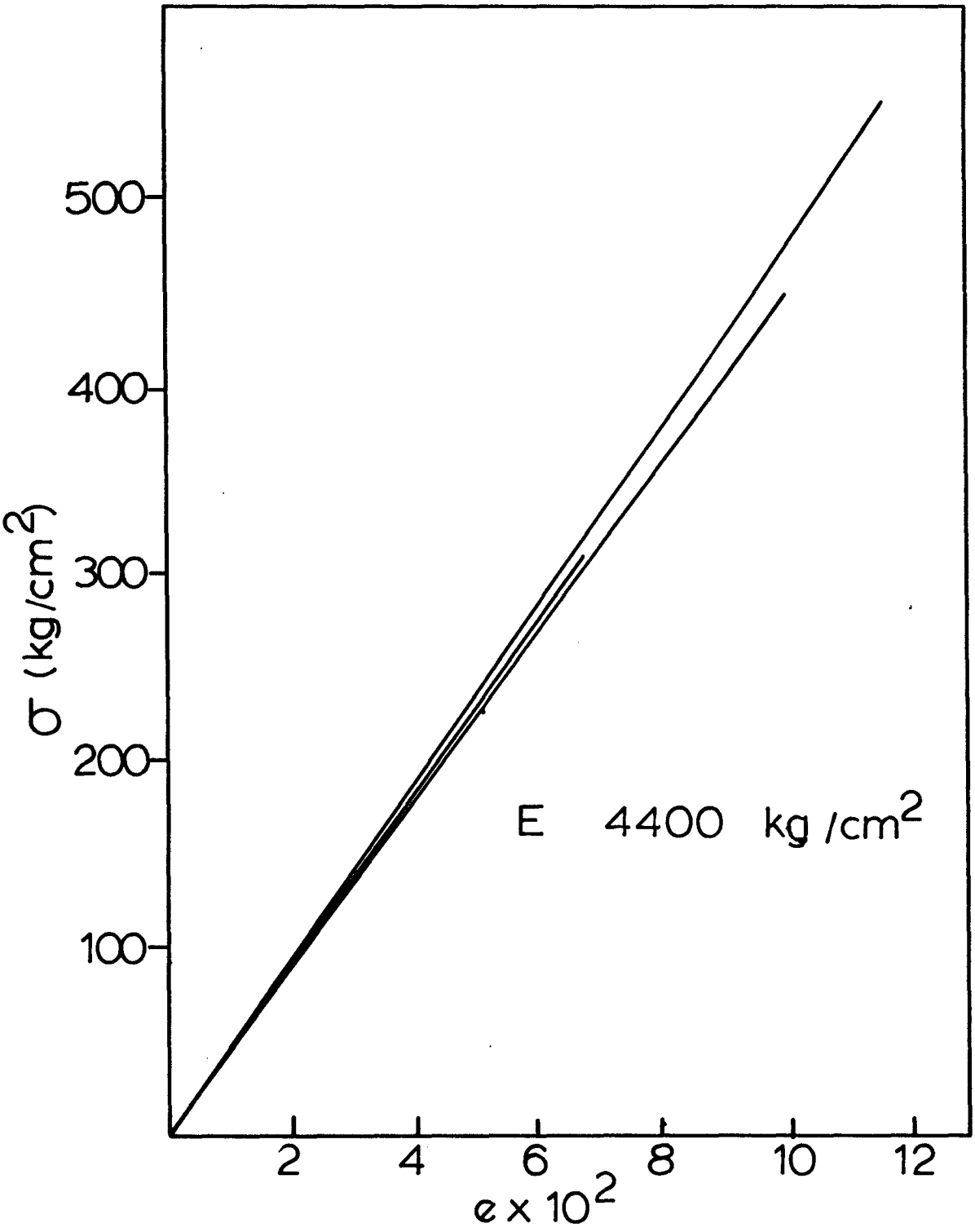

Figure 21

Stress Strain Curve of PE 31575

P-1500 psi

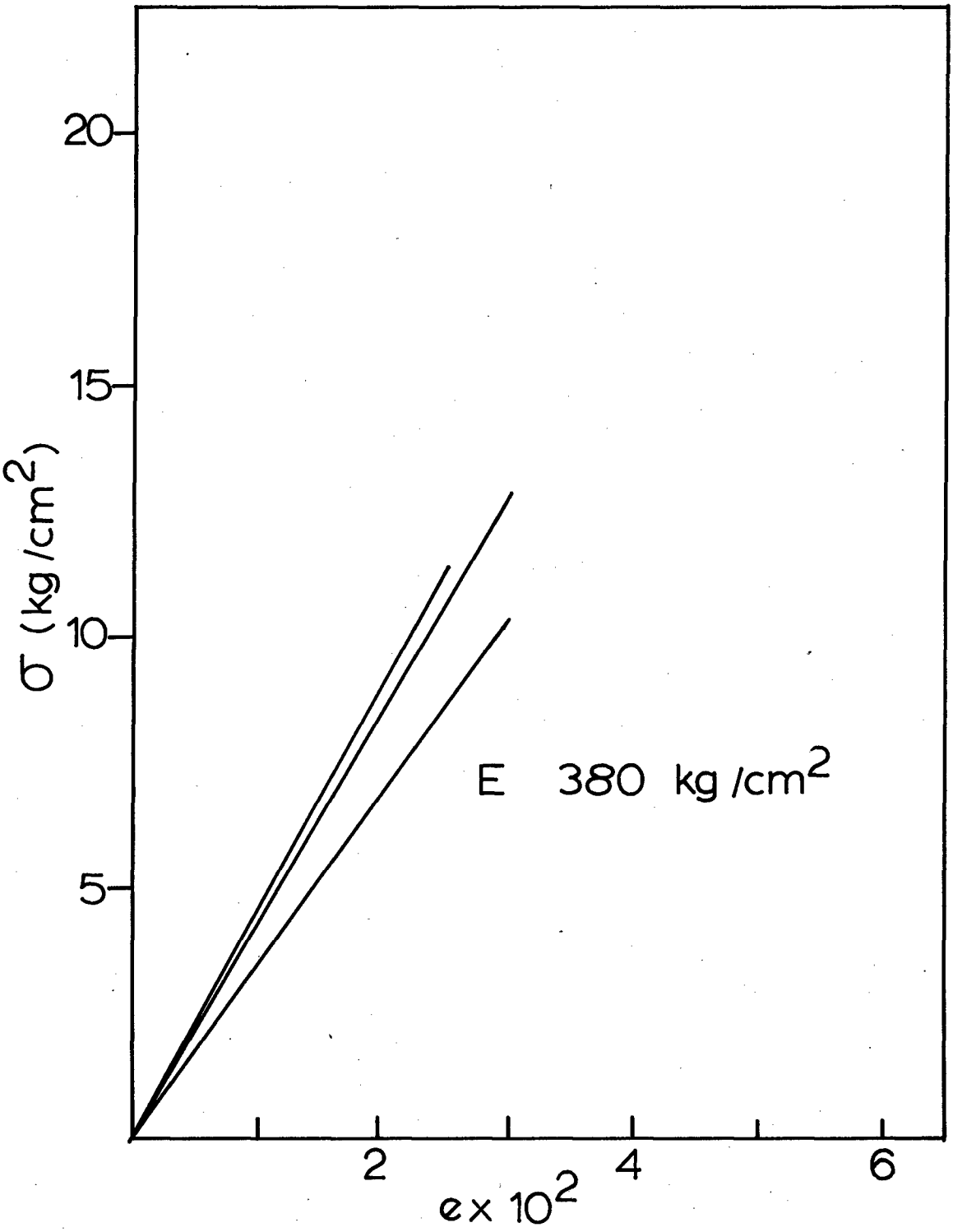

Figure 22

Stress Strain Curve of PE 3475

P-2000 psi

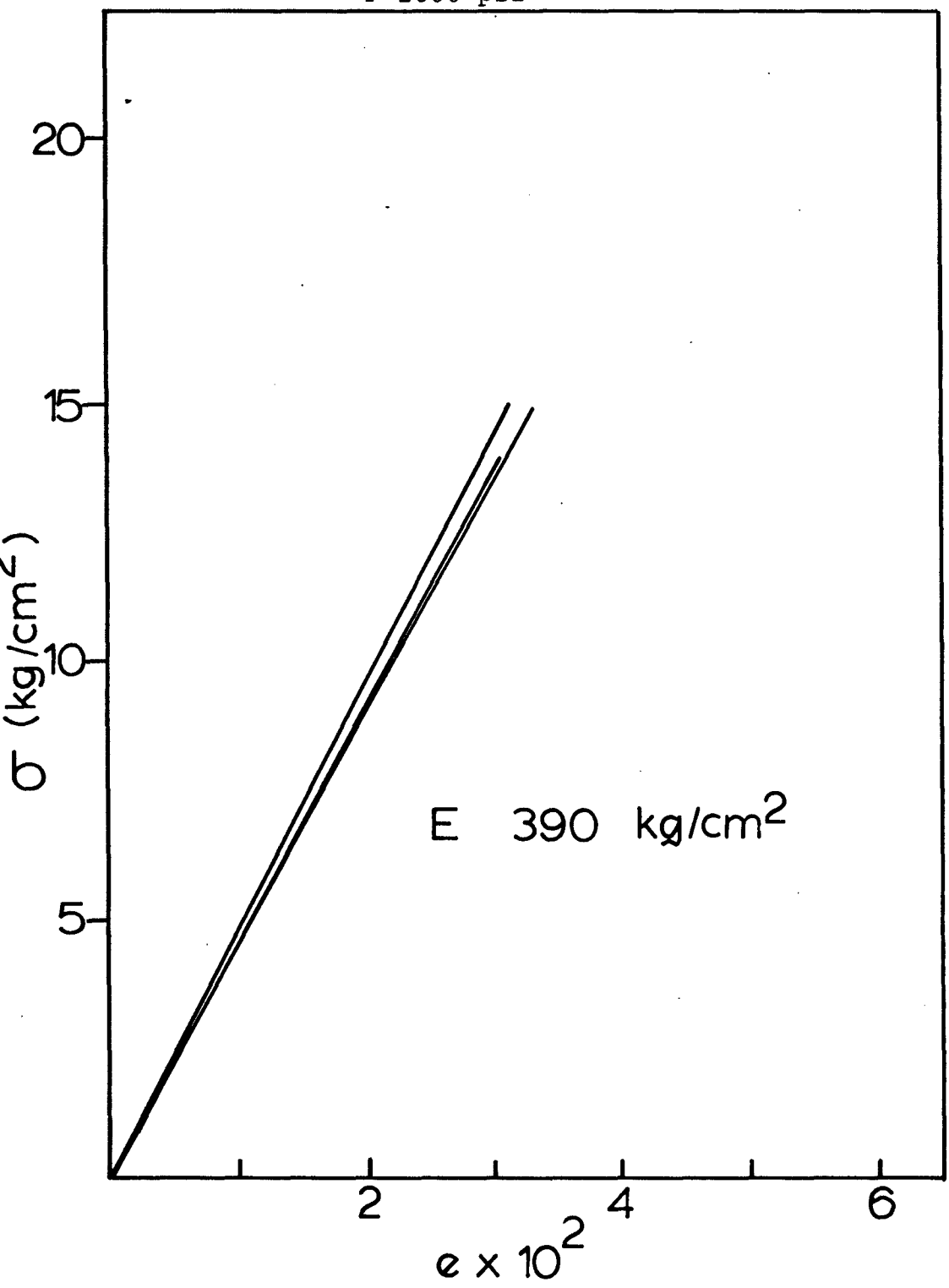

Figure 23

Stress Strain Curve of PE 22075
P-3000 psi

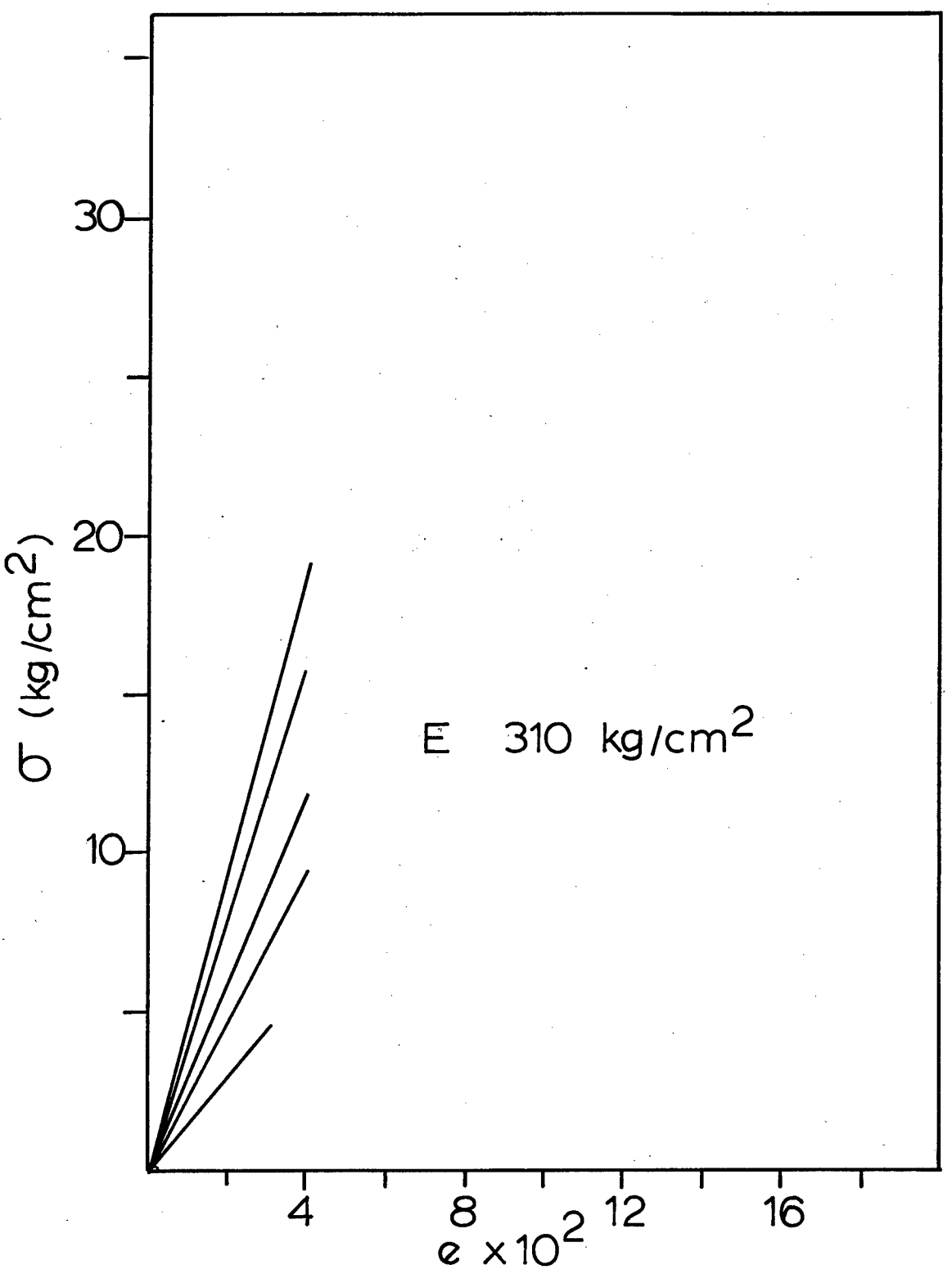

Figure 24

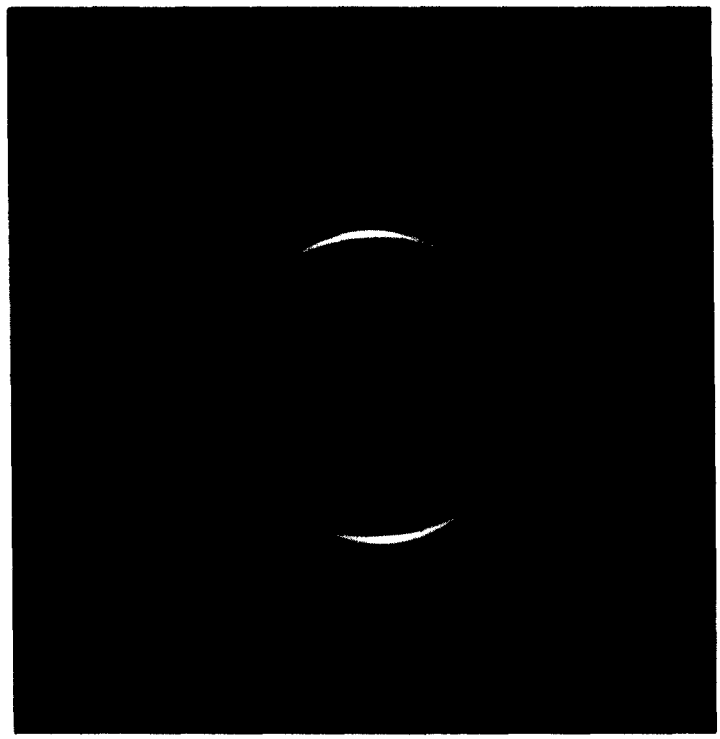

Wide Angle X-Ray Diffraction Pattern of PE

(500 psi)

Figure 25

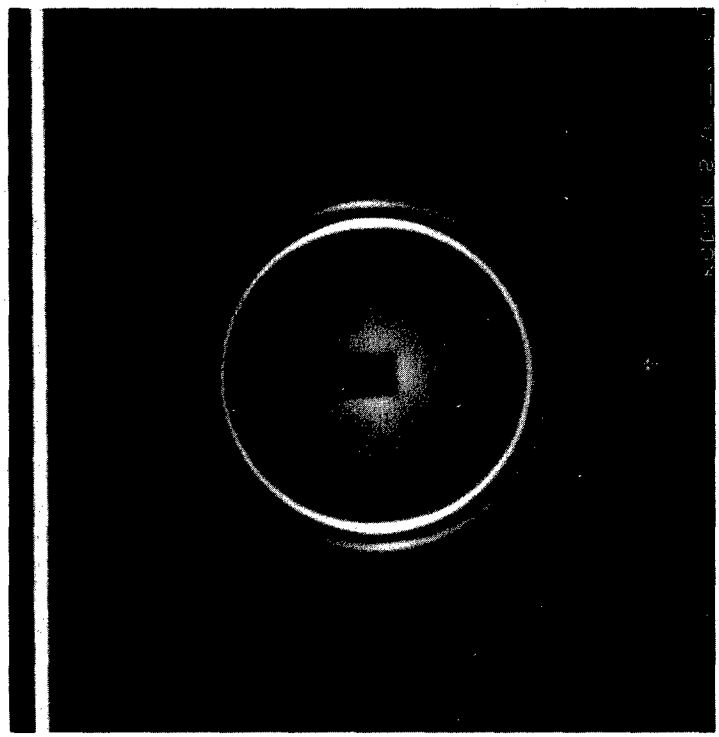

Wide Angle X-Ray Diffraction Pattern of PE

(1500 psi)

Figure 26

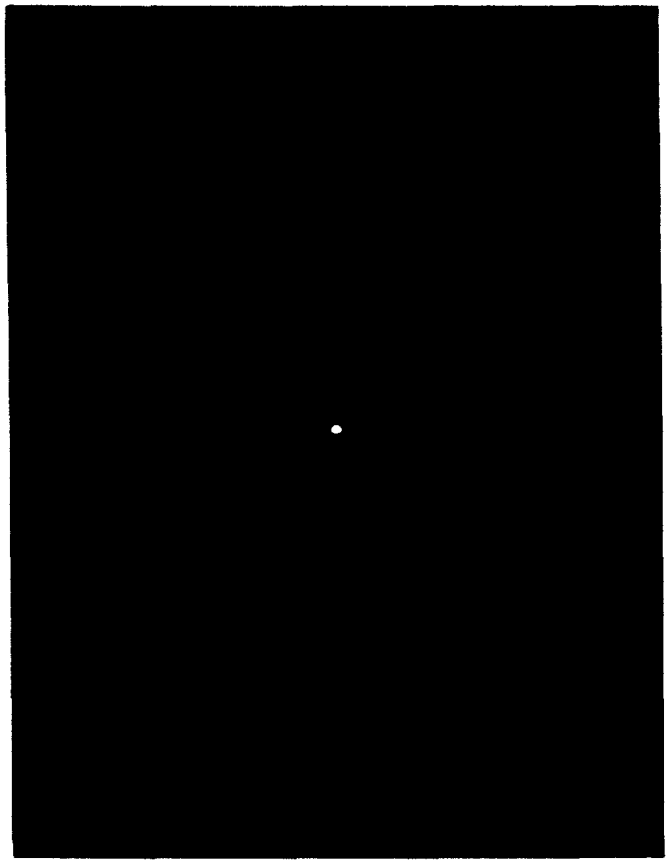

Wide Angle X-Ray Diffraction Pattern of PE

(2000 psi)

Figure 27

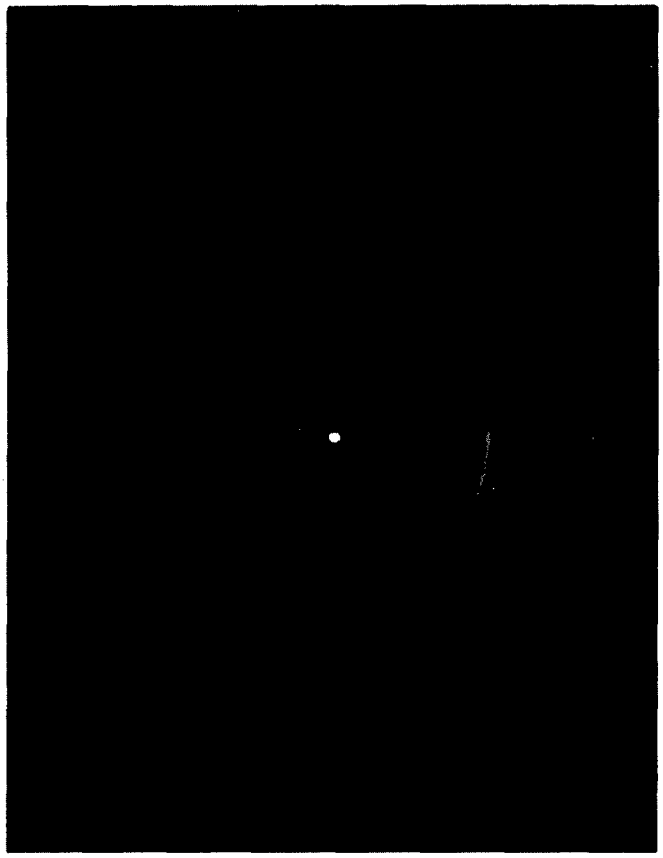

Wide Angle X-Ray Diffraction Pattern of PE

(3000 psi)

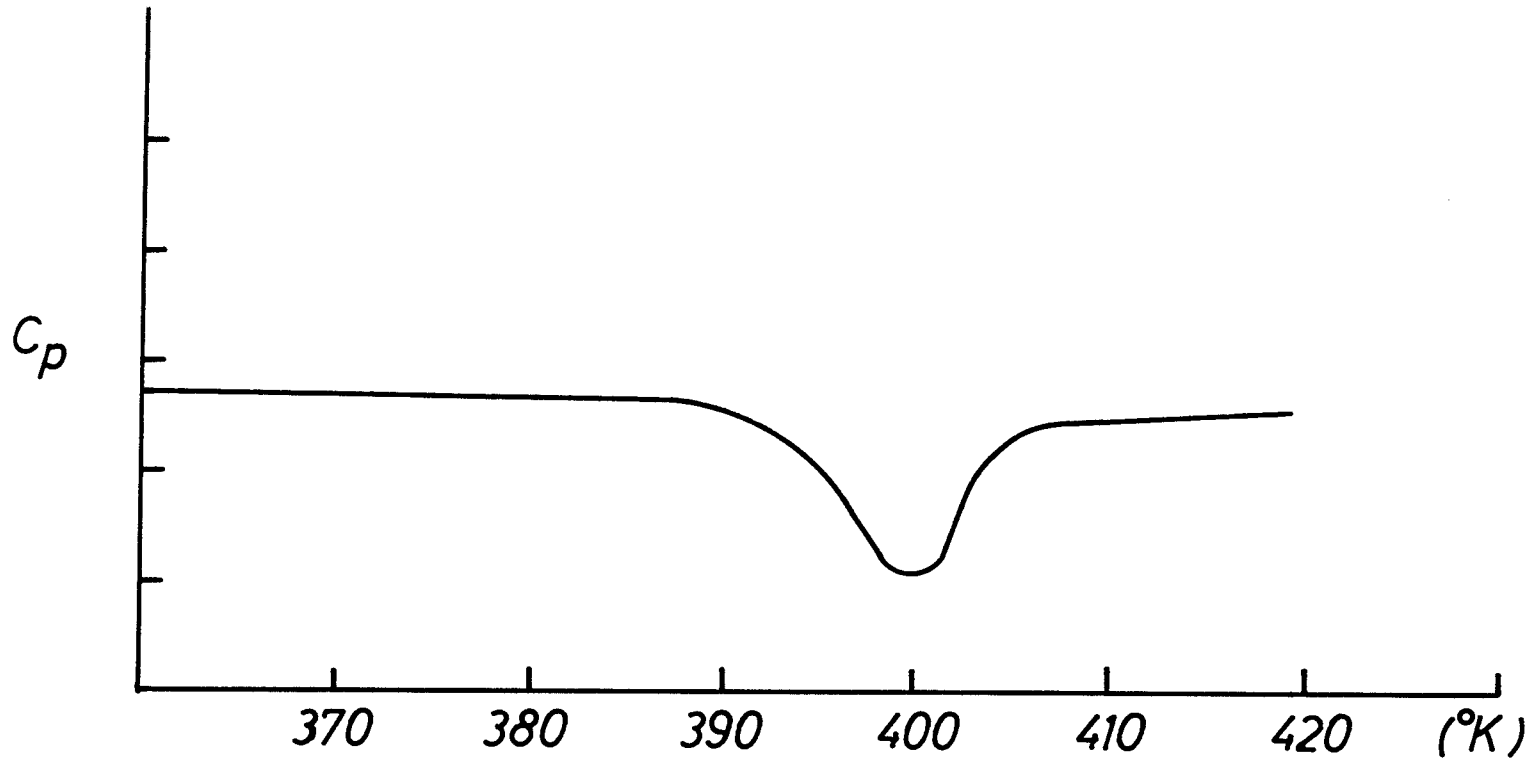

Fig. 28
DSC Trace of PE-0. The amplitude is proportional to heat capacity (cal /deg-mole) X = 54.4 %

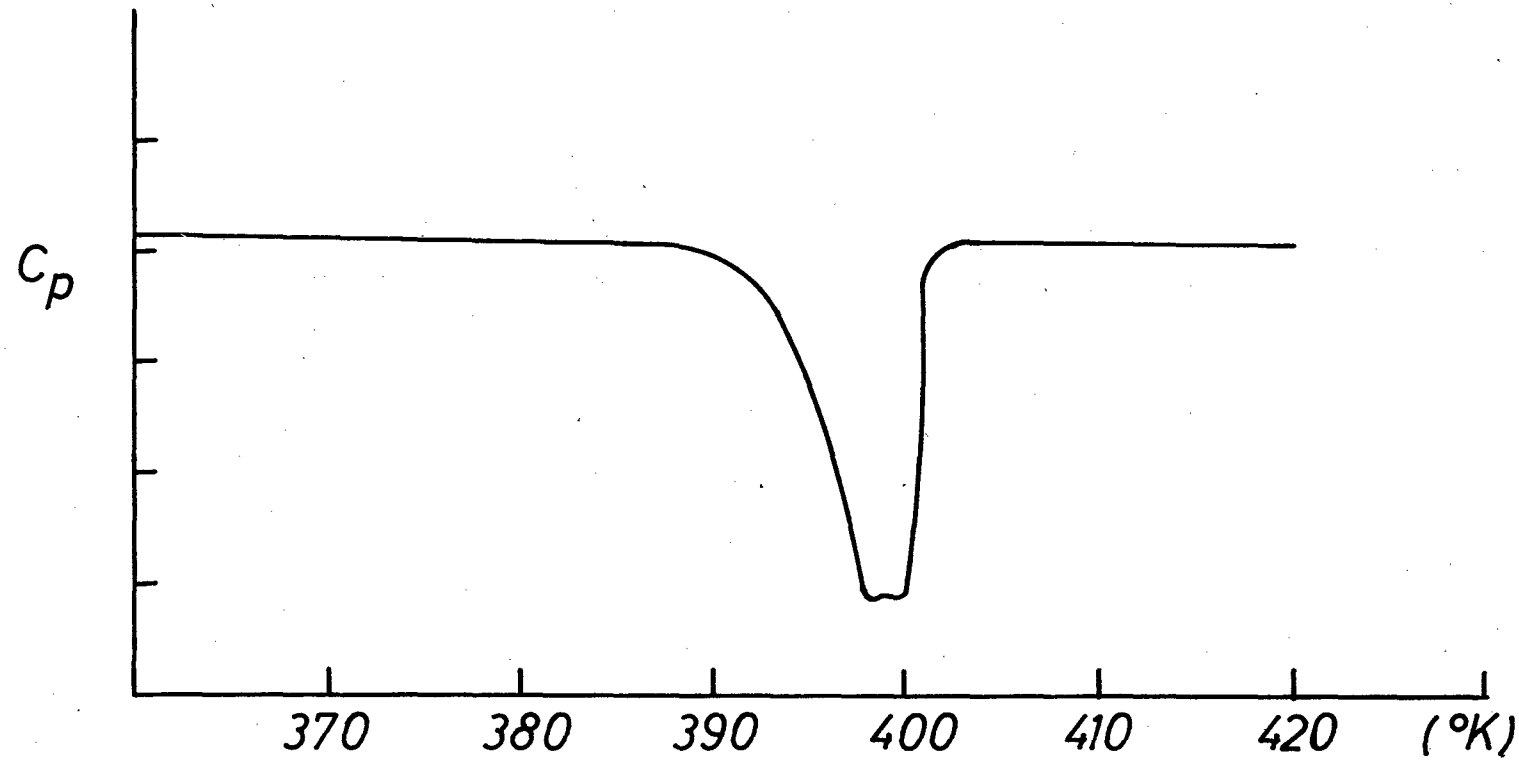

Fig. 28

DSC Trace of PE 5. The amplitude is proportional to heat capacity (cal/deg-mole).

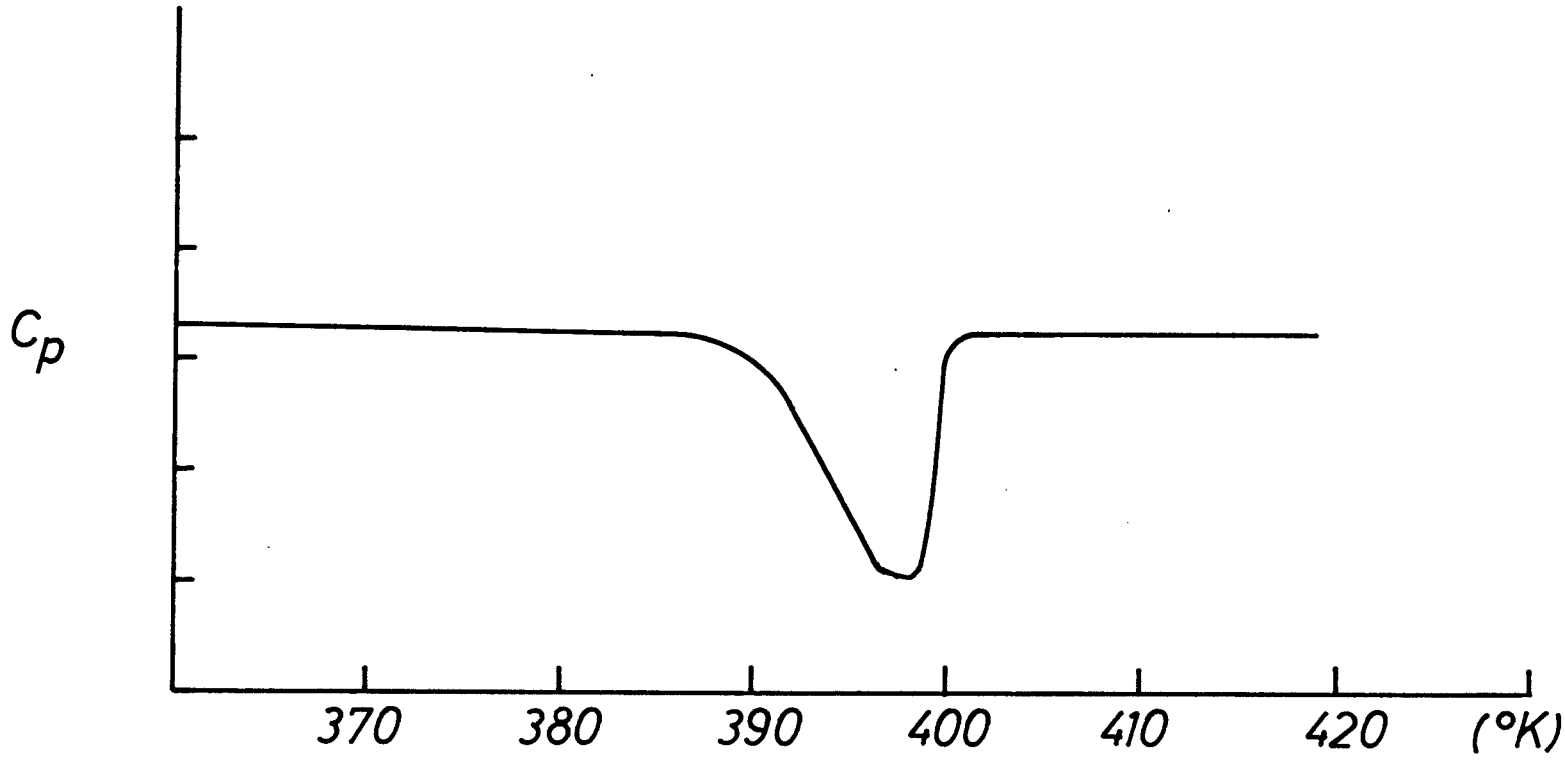

Fig. 30
DSC Trace of PE 10. The amplitude is proportional to heat capacity (cal/deg-mole). X= 68.4%

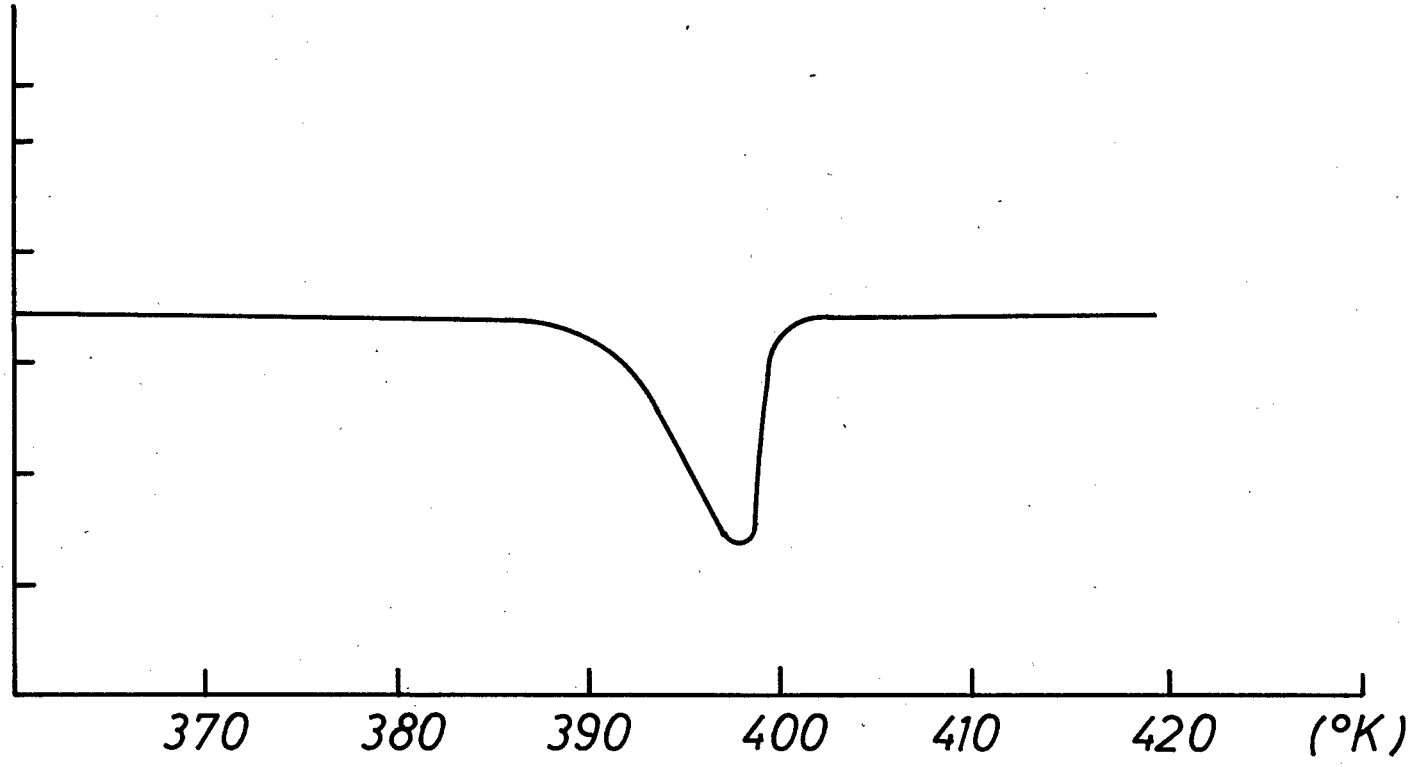

Fig 31

DSC Trace of PE 20 The amplitude is proportional to heat capacity (cal /deg-mole) X = 78.5 %

Figure 32a

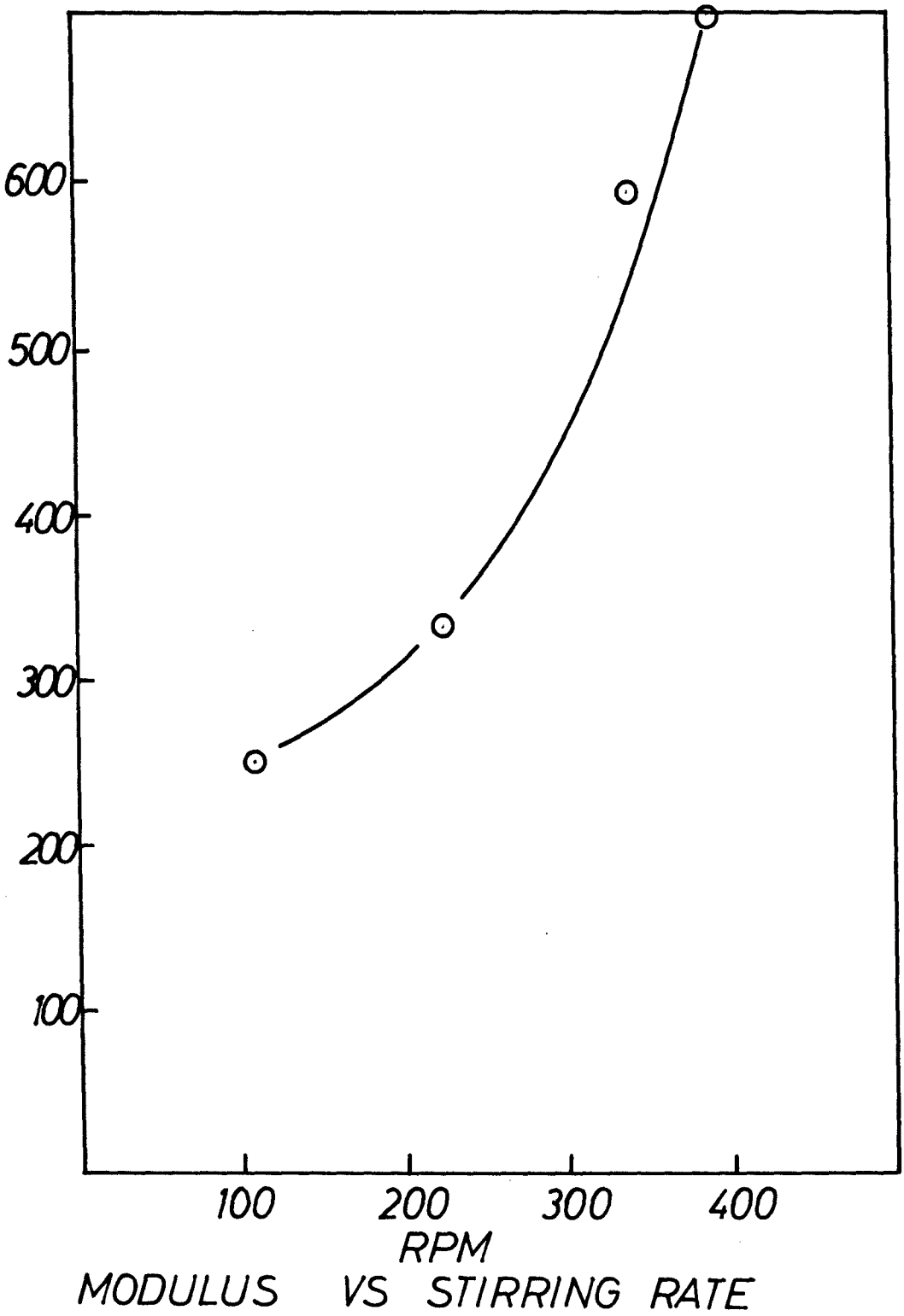
600
500
400
300
200
100
100
200
300
400
RPM
MODULUS VS STIRRING RATE

Figure 32b

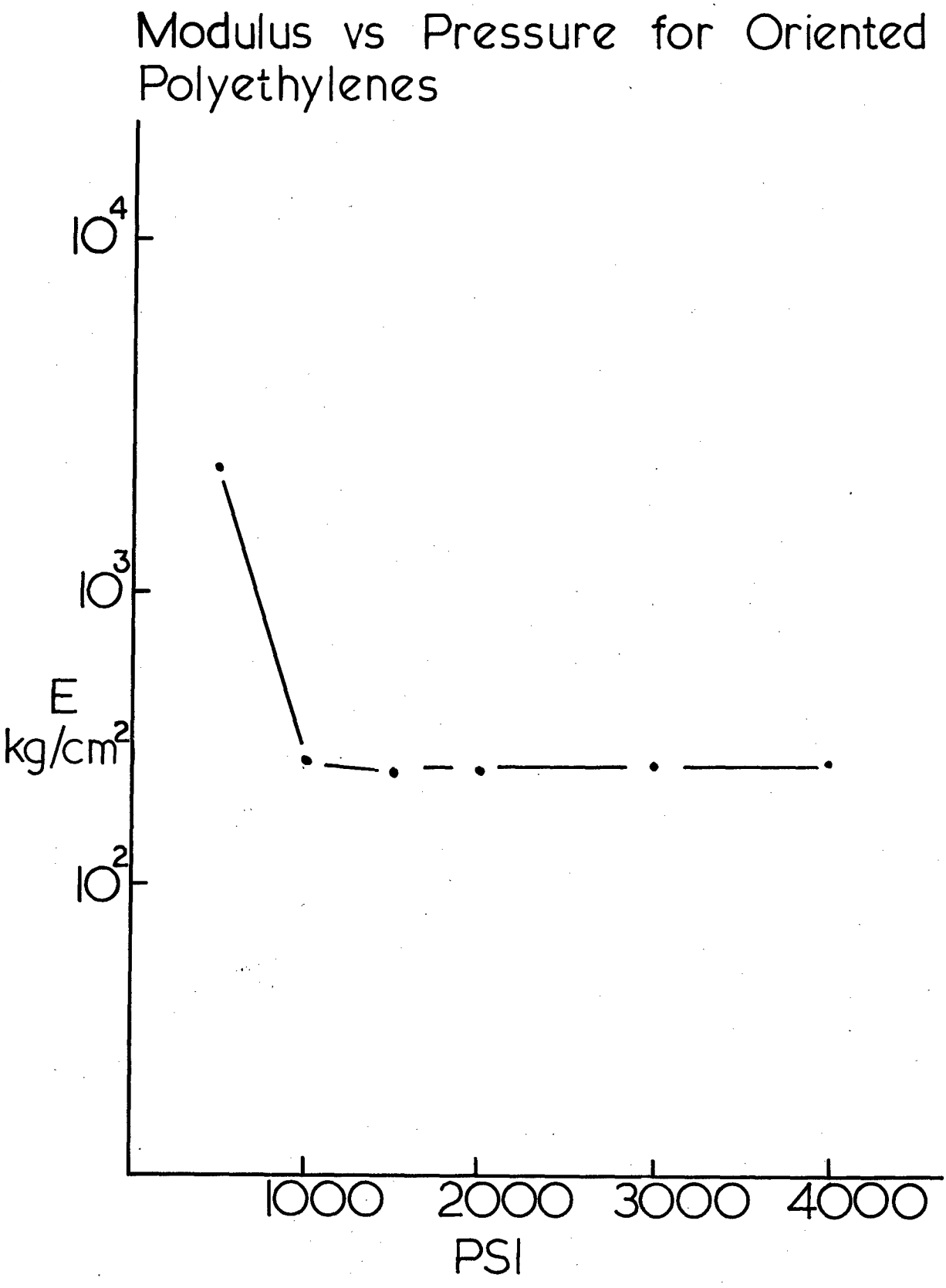
Modulus vs Pressure for Oriented Polyethylenes
10^4
10^3
10^2
E
kg/cm^2
1000
2000
3000
4000
PSI

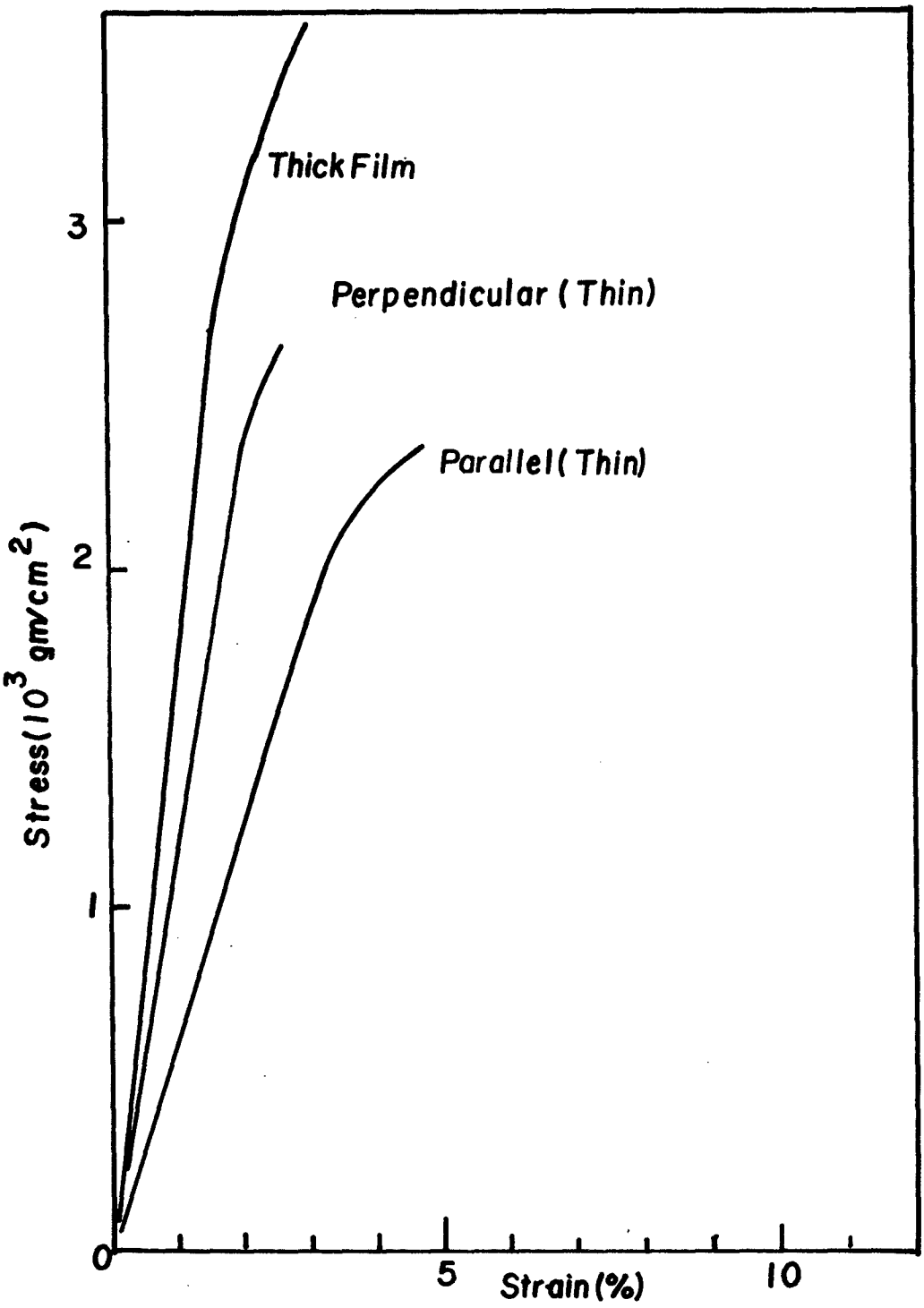

Fig 33 Stress - Strain Curves of Polystyrene (260,000Mw) Films

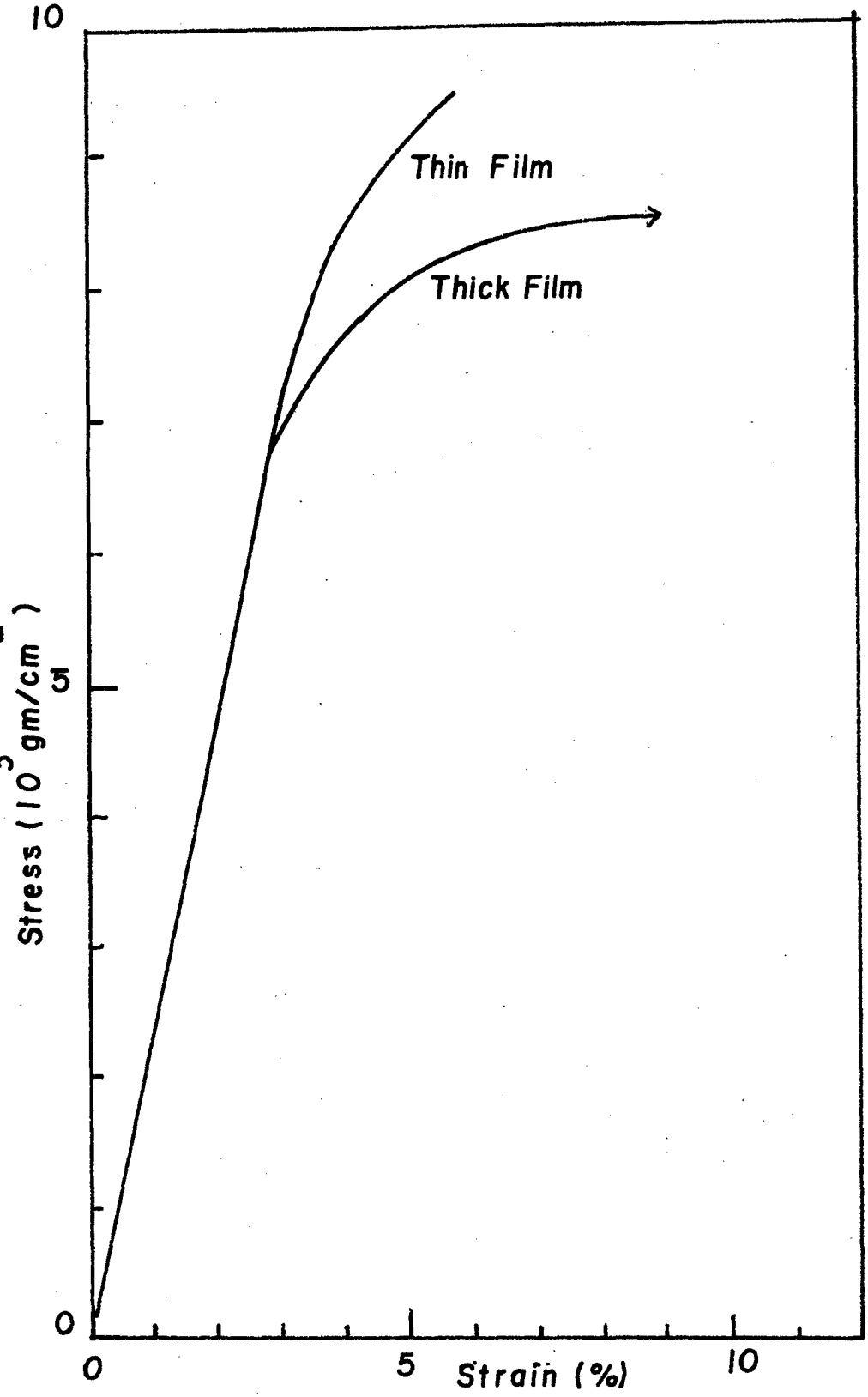

Fig 34 Stress-Strain Curves of Cellulose Acetate Films

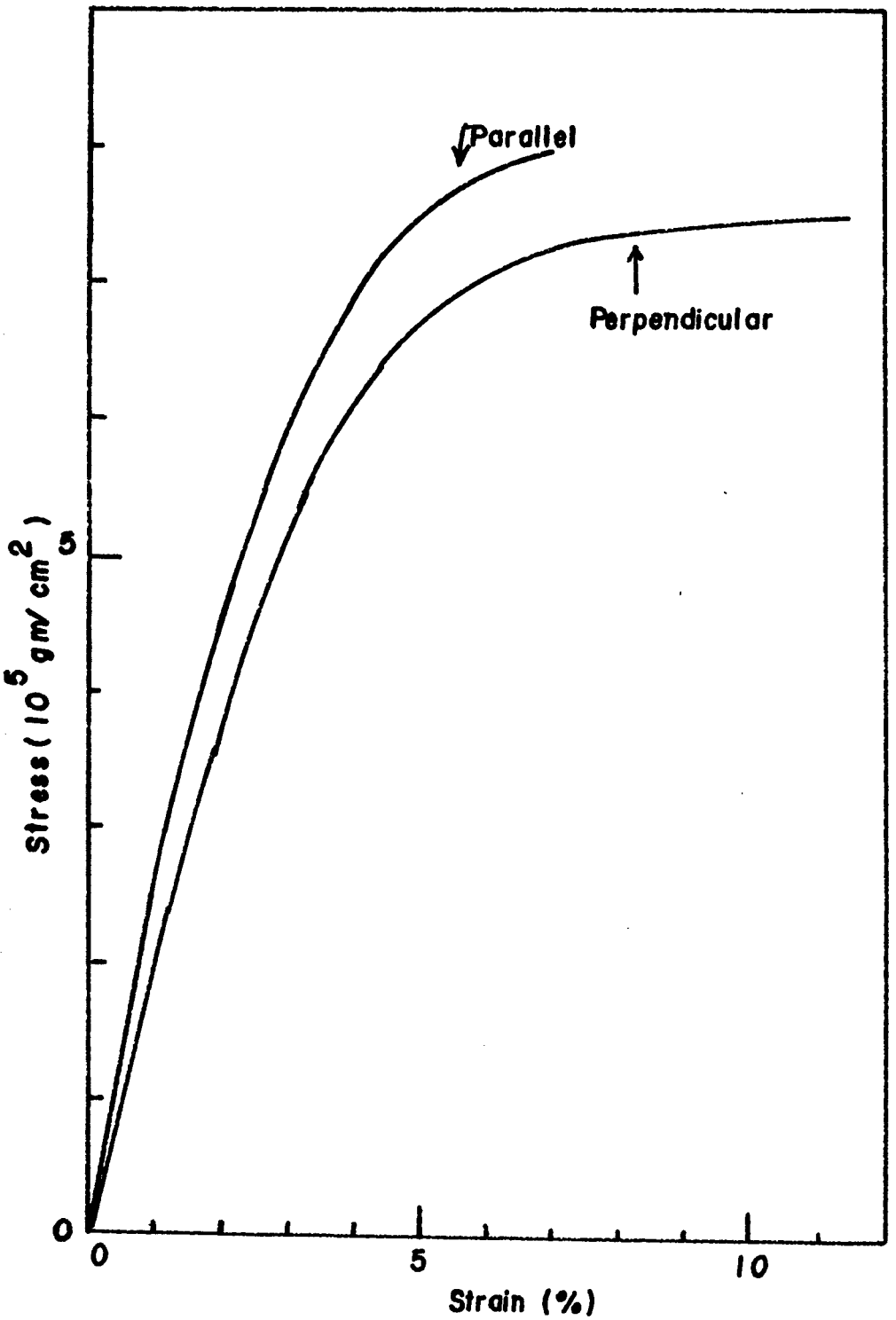

Fig. 35 Stress-Strain Curves of Cellulose Acetate Thin Film

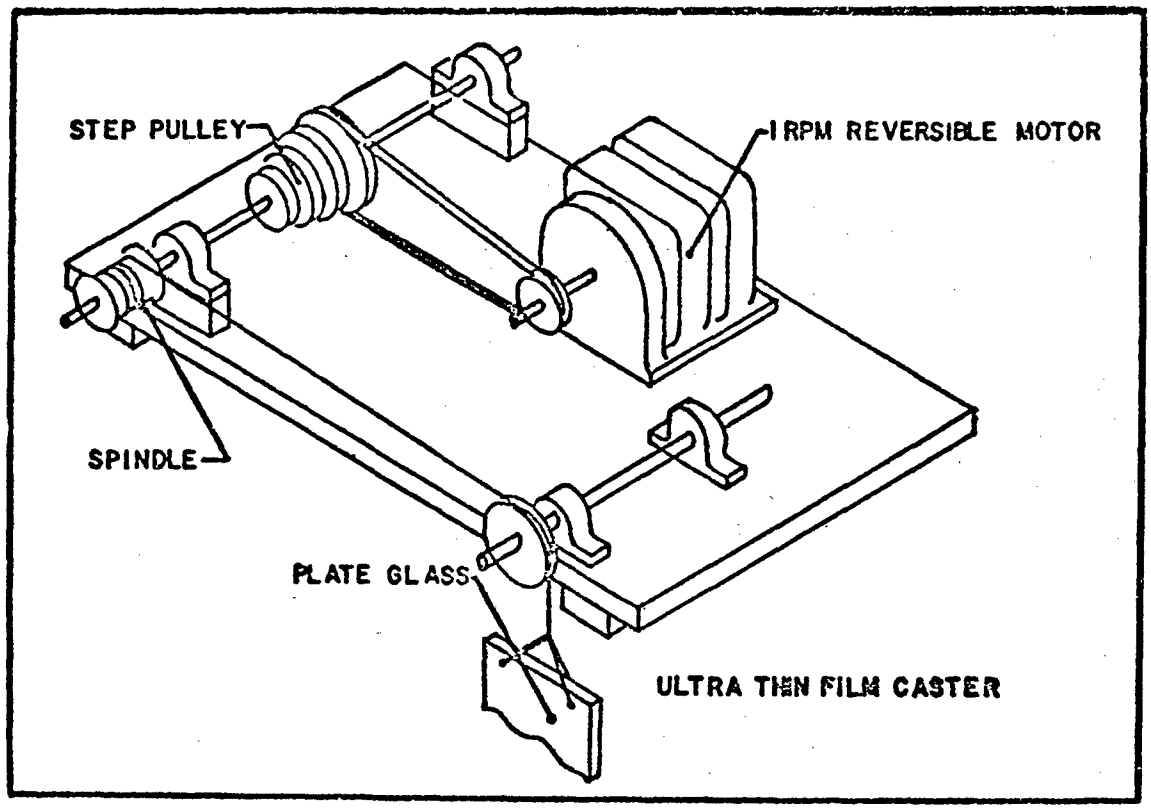

FIGURE 36 ULTRA THIN FILM CASTER

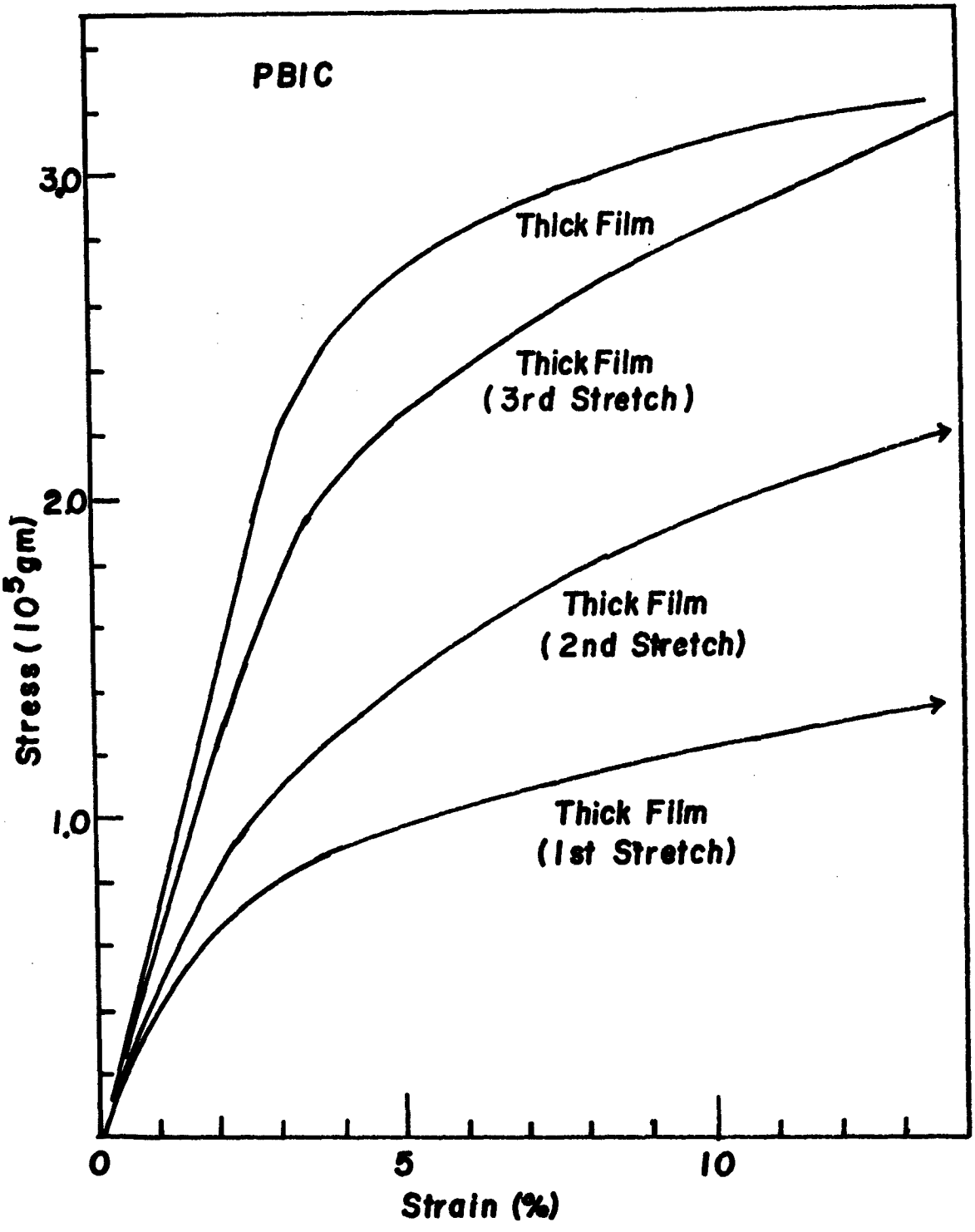

Fig 37 Stress–Strain Curves of PBIC FILMs

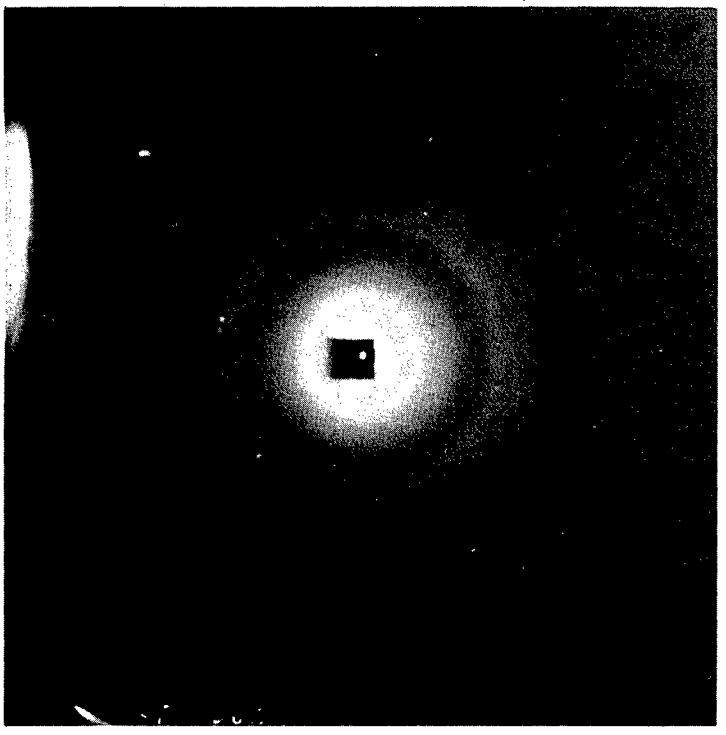

Figure 38. X-Ray Picture PBIC
Thin Film

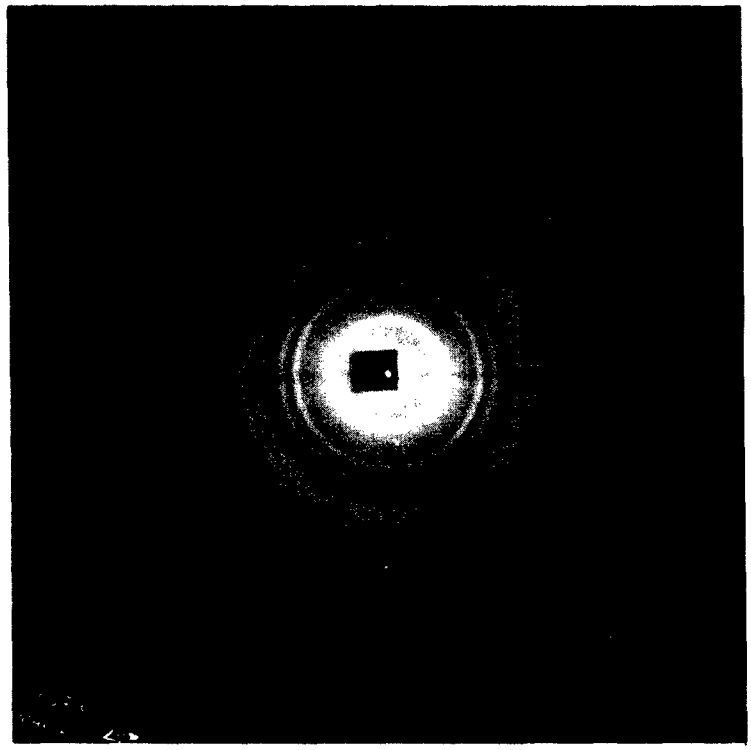

Figure 39. X-Ray Picture PBIC
Thick Film

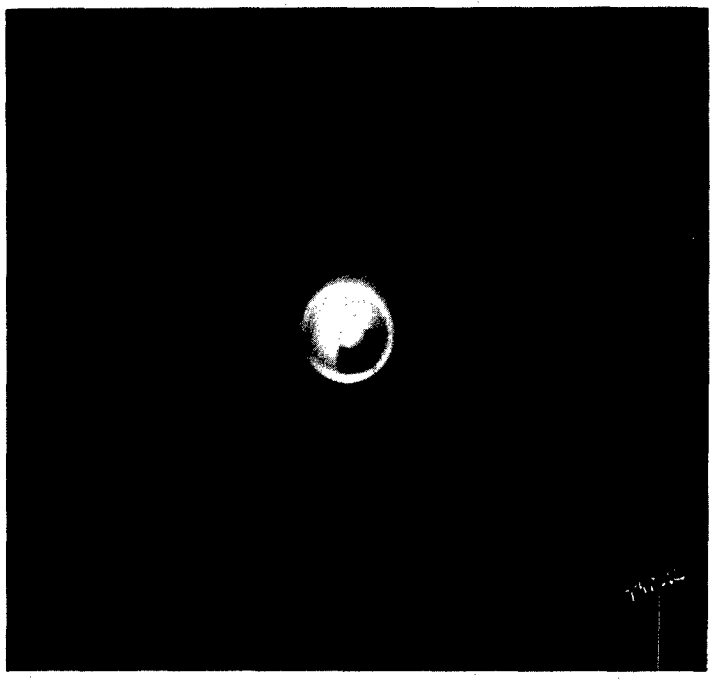

Figure 40. X-Ray Picture PBLG

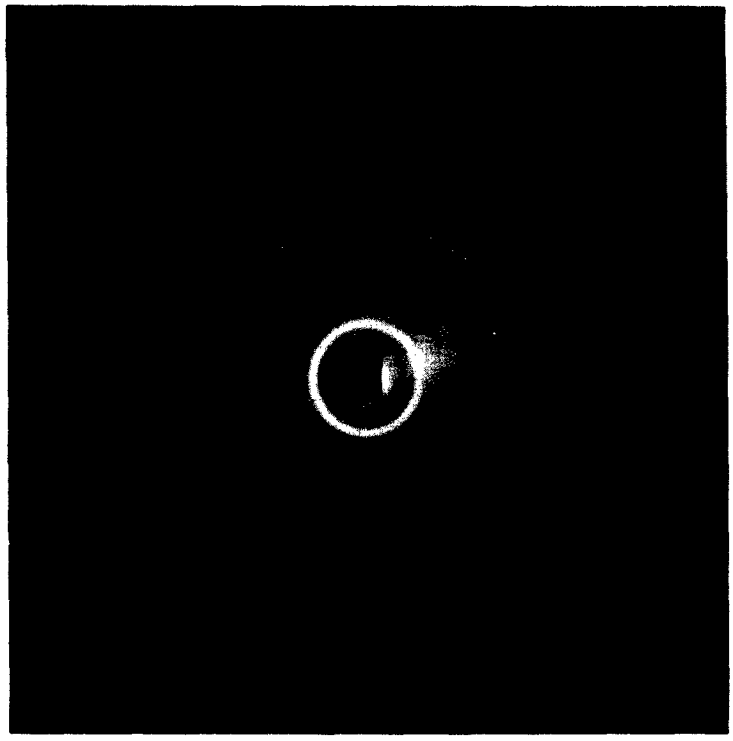

Figure 41a. X-Ray Picture PBIC-Melt

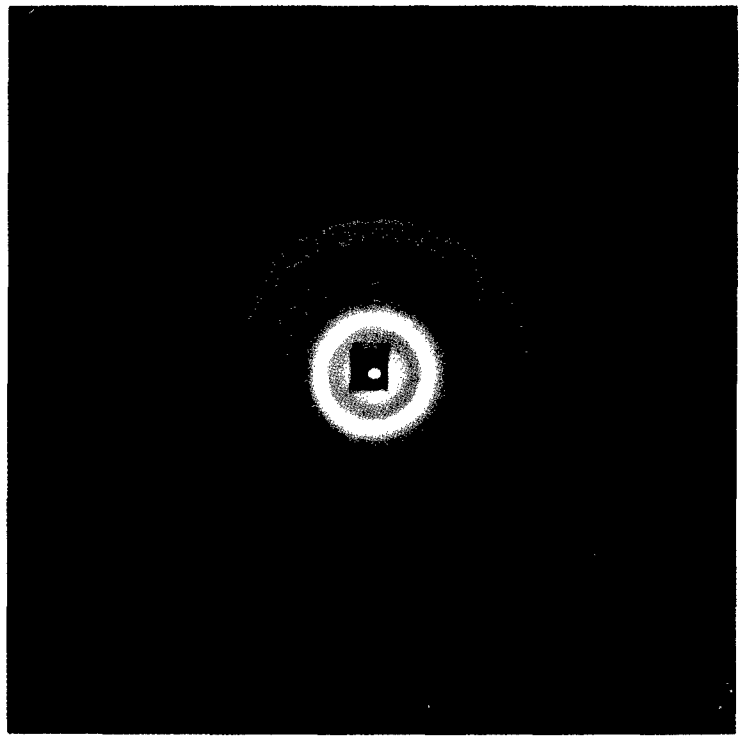

Figure 41b. X-Ray Picture PBIC-Random

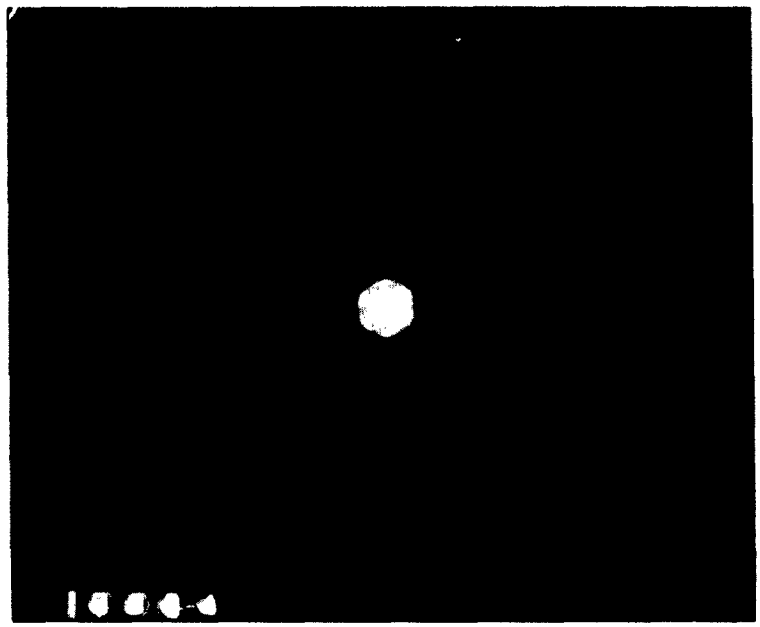

Figure 42. Electron Diffraction
PBIC

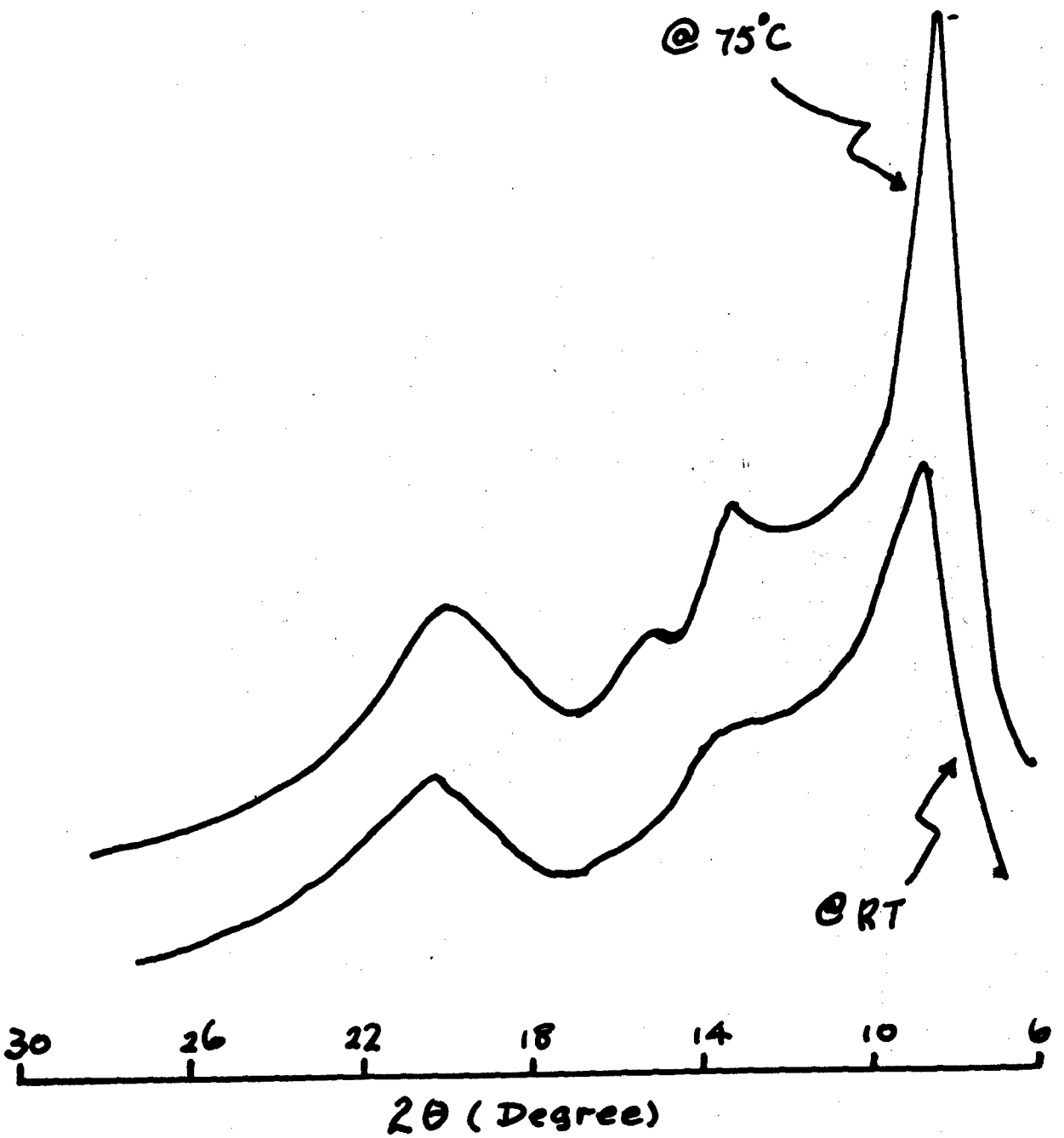

Figure 43. X-Ray Diffraction as a Function of Temperature

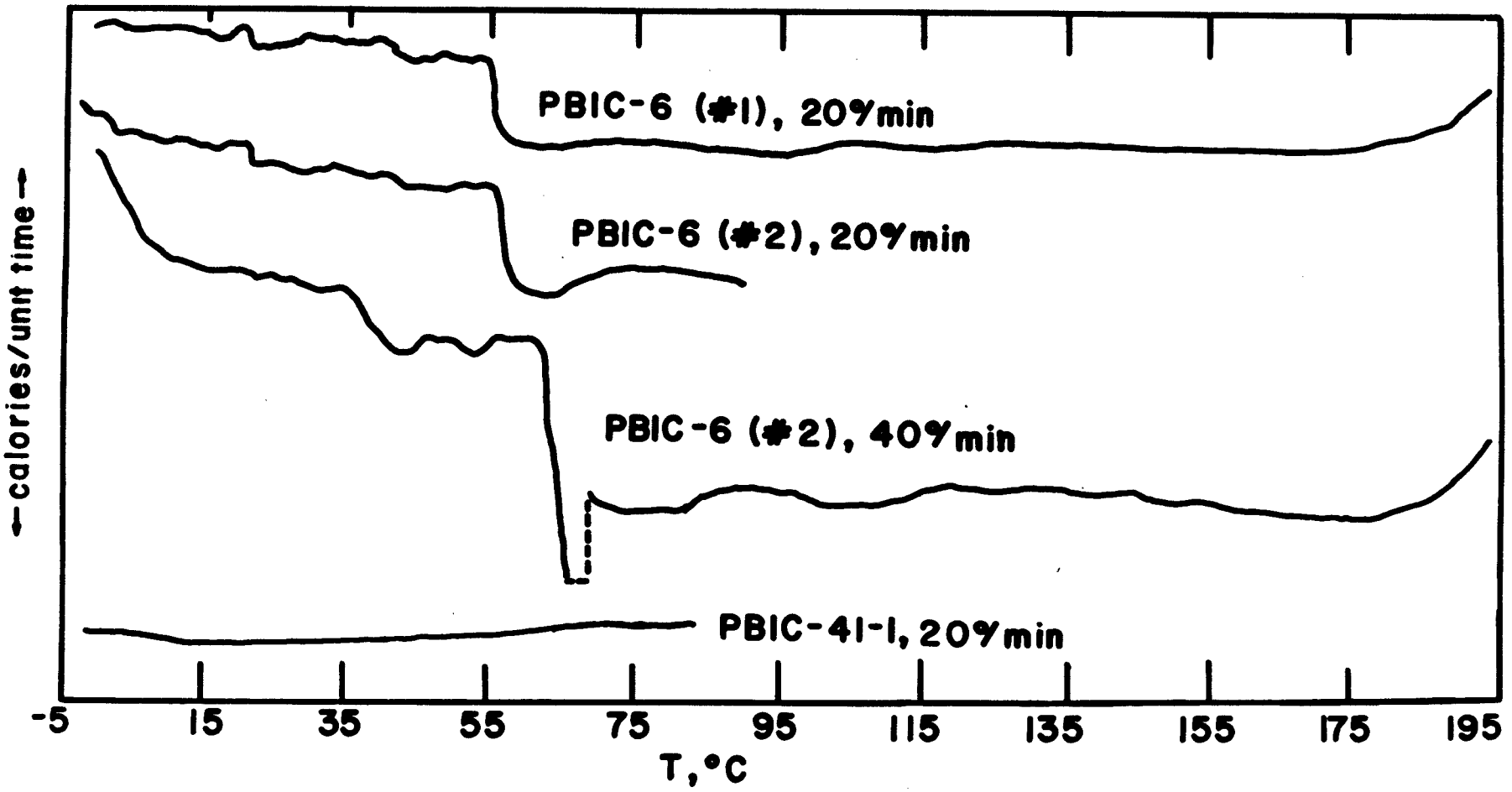

Figure 44. Thermal Analysis (DSC) of PBIC

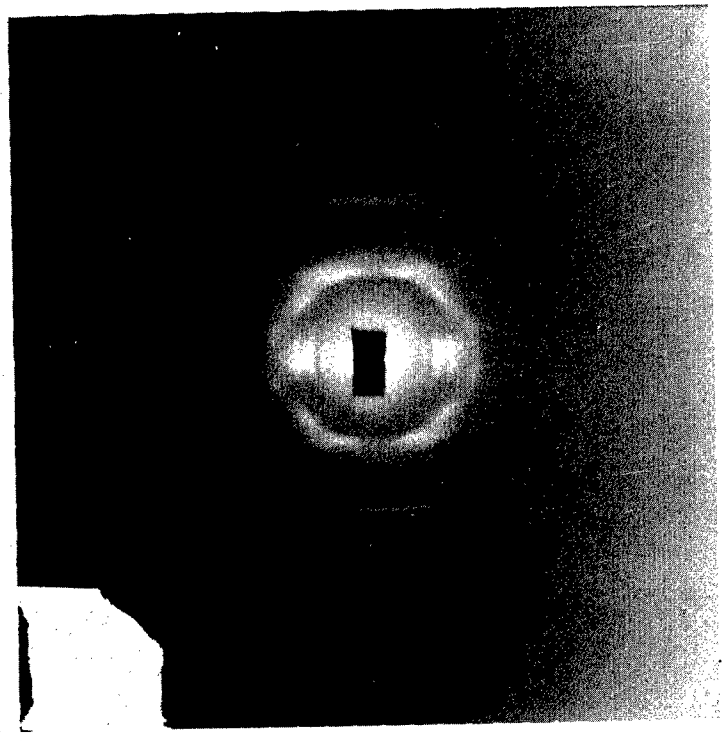

Figure 45. X-Ray Picture
PHIC-fiber

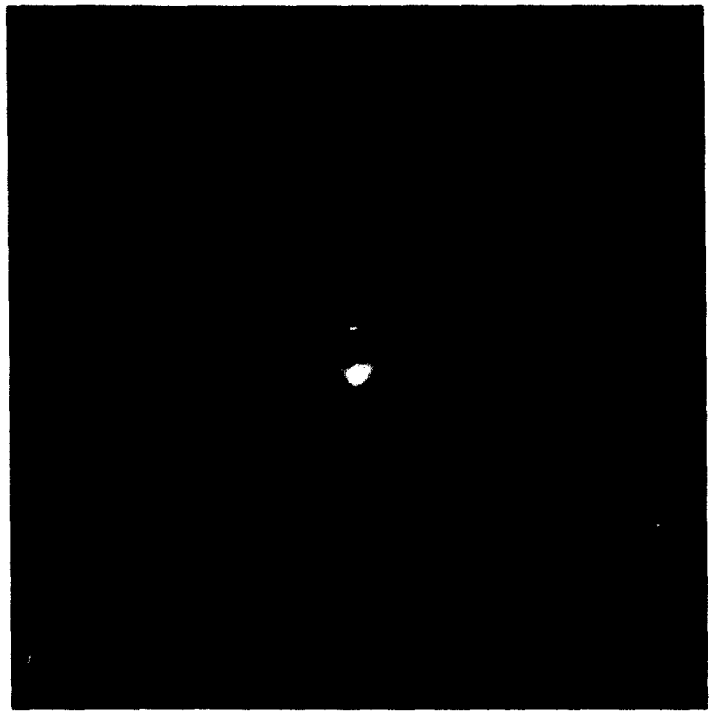

Figure 46. X-Ray Picture
POIC-fiber

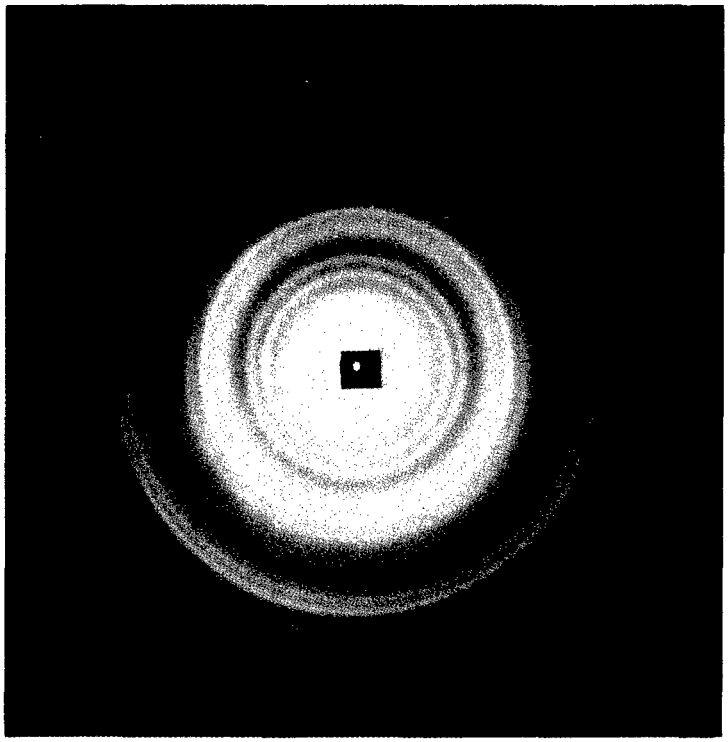

Figure 47. X-ray Picture
POIC-Random

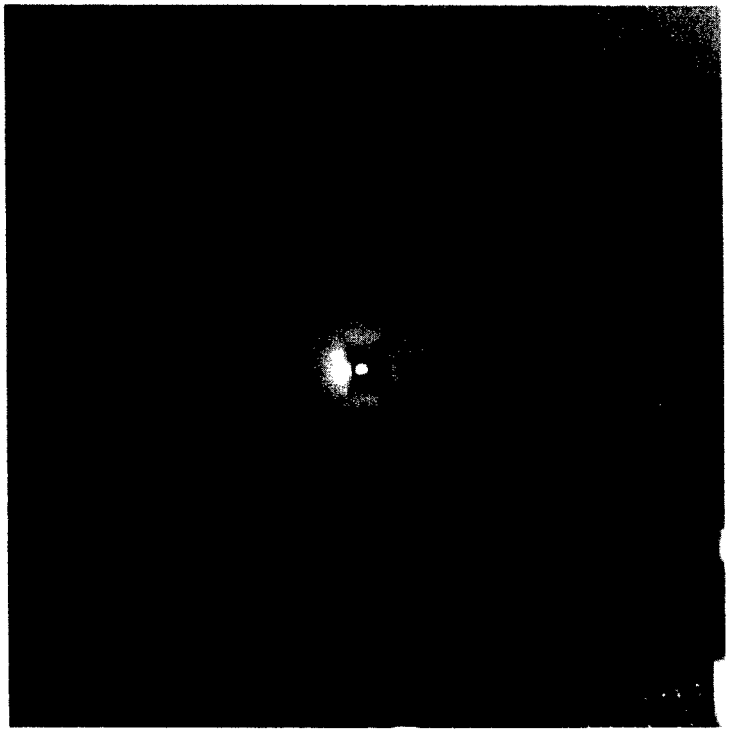

Figure 48. X-Ray Picture Kevlar
Thin films, as cast

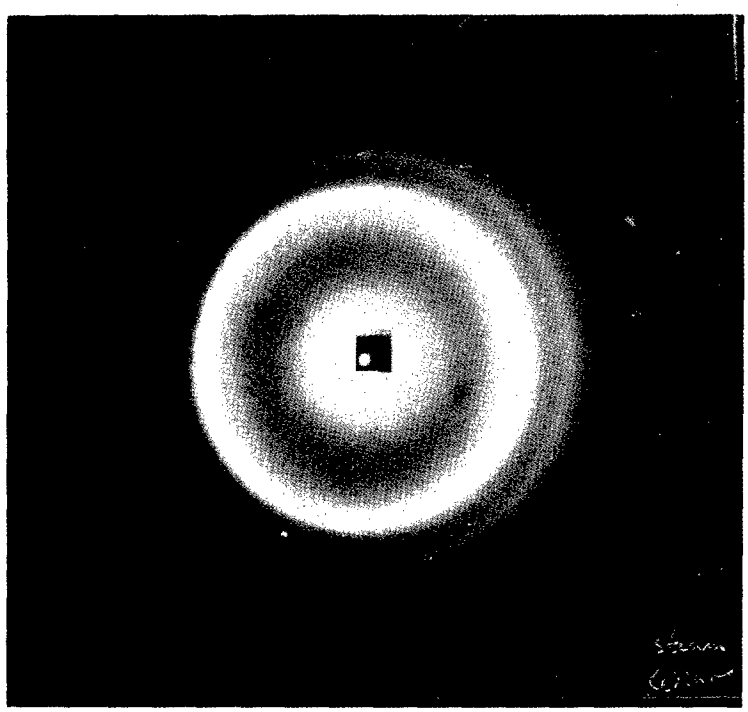

Figure 49. X-Ray Picture Kevlar-
Steam annealed

☆ U. S. GOVERNMENT PRINTING OFFICE: 1976 — 657-630/645